

Geometrical aspects of the interaction between expanding clouds and environment

F. Spineanu,^{1, a)} M. Vlad,¹ and D. Palade¹

*National Institute of Laser, Plasma and Radiation Physics Bucharest,
Romania*

(Dated: August 2, 2021)

This work is intended to be a contribution to the study of the morphology of the rising convective columns, for a better representation of the processes of entrainment and detrainment. We examine technical methods for the description of the interface of expanding clouds and reveal the role of *fingering* instability which increases the effective length of the periphery of the cloud. Assuming Laplacian growth we give a detailed derivation of the time-dependent conformal transformation that solves the equation of the *fingering* instability. For the phase of slower expansion, the evolution of complex poles with a dynamics largely controlled by the Hilbert operator (acting on the function that represents the interface position) leads to *cusp* singularities but smooths out the smaller scale perturbations.

We review the arguments that the rising column cannot preserve its integrity (seen as compacity in any horizontal section), because of the penetrative downdrafts or the incomplete repulsion of the static environmental air through momentum transfer. Then we propose an analytical framework which is adequate for competition of two distinct phases of the same system.

The methods examined here are formulated in a general framework and can be easily adapted to particular cases of atmospheric convection.

PACS numbers: 52.55.Fa, 52.20.Dq, 52.25.Fi

^{a)}florin.spineanu@euratom.ro

I. INTRODUCTION

In the atmospheric convection leading to cumulus clouds there is a continuous exchange of heat and water (vapor, liquid) between the rising column and the environmental air. This problem is complex and has been examined by observation, analytical theory and numerical simulation^{4, 7, 6, 29, 28}. The diversity of situations cannot be captured by a unique model.

The rate of exchange depends, besides many other factors, on the geometry of the contact interface between the two gaseous media. Part of the interaction with the environment takes place at the periphery of the cloud, an interface that evolves and is subject to geometric instabilities. In the expanding phase the small scale structure is determined by instabilities of the *fingering* type. Like in the case of the Hele-Shaw instability, one can map the physical problem on a time-dependent conformal transformation to a fixed complex line. At small scale, there can be random fluctuations due to the background turbulence. The effective length of contact between the cloud and the environment is then much greater than the perimeter of *hull* of the cloud in horizontal plane. This enhances the transport between the two neighboring gaseous media.

In the phase where the expansion slows down (the input from the rising flux is reduced) the small scale profiles (resulted from “fingering” and random fluctuations) are smoothed out by a process of attraction and alignment of the complex poles that define the solution. The result is that the interface exhibits *singularities* of a special type, *cusps*. They occur through coalescence of small scale quasi-singular perturbations of the wrinkled interface. If the time evolution leads to self-intersection of the interface, a parcel of environmental air is simply swallowed into the expanding cloud.

Finally, inside the rising column there is interaction between the cloud air and the environmental air that either remains by breaking the initially compact rising column, or penetrates from above as downdrafts on long vertical distances.

This last case requires few comments. There are various forms of contact between the two gaseous media that are in relative motion. In a simplified descriptive picture we can see the rising column as a stream of gas with specific properties penetrating a volume of stationary gas (static environmental air) with different properties. If the speed of the stream is high, there is transfer of momentum from the stream to the the environmental air through

collisions at the front of contact, *i.e.* at the top of the rising column. Then the environmental air is deflected (pushed up and sidewise) and the body of the column preserve its properties.

Alternatively, if the linear momentum of the rising column is small, then the stream of the convective air cannot repulse through momentum transfer the environmental air and there is easier interpenetration of the two gases. The rising stream is teared apart and elements of the air of the column are interspersed between elements of the environmental air and this occurs up to small spatial scales, of the turbulence. Obviously, the exchange of heat and water (vapor and liquid) is much more efficient in this case. This is the case of either shallow convective events that are dissipated before becoming a buoyant column or (and this is most interesting) of clouds in the last phase of their ascent where the vertical advancement is slowed down and elements of the cloud are dispersed in the environment.

For a comparison, the two cases have been found experimentally in the expansion of a laser-generated plasma in a low density plasma². With variation within a range of parameters the interaction changes from interpenetration to formation of an interface.

These two situations are limiting cases. In general it is expected that the rising convection columns that form the cumuli are characterized by strong buoyancy that allows them to reach high altitude. Therefore they are closer to the first case described above, where the stream is able to push off (out of) its way the environmental air and the contact with this one mainly takes place at the moving top and at the circumference. Even if the vertical momentum of the rising column is high, the possibility to retain a compact structure is improbable. More realistic is the expectation that the initially compact column will break up into streams separated by irregular but vertically-connected volumes (channels) of static environmental air. In short, the breakup of the rising column leaves open spaces inside the initially compact area and in these spaces there still is static environmental air. The transfer of mechanical momentum from the rising cloud air to the static environment is mediated by exchange of turbulent eddies, therefore implicitly involves dilution of cloudy air and evaporative cooling for the environmental air. This occurs mainly at the top of the rising column. Parcels of the cooled environmental air will descend and will push the still un-mixed environmental air present in the contiguous channels remaining inside the broken column. The mass conservation requires the environment to respond to the rise of the convective air by currents of descending air, which takes place in a layer around the rising column but also in the spaces left open after the breakup of the rising column. Therefore, elements of rising

air that are at a certain level height will be in close contact with environmental air that, actually, originates at levels of height that are much above the current level and are *not* yet mixed with cloud air. Then the *mixing* will take place at various heights. This picture is very close to what is observed in a classical Reyleigh-Benard system in the transitory phase where the purely conductive state is going to be replaced by the convective state. This bifurcation is preceded by emission of thermal streams (plumes) at the hot plate, which do not have the chance to produce a full scale convection. However they are able to determine thorough mass and momentum conservation, generation of opposite streams, originating at the cold plate and descending. There is no mixing between the rising and descending plumes except at late stages, when the convection span the whole volume. Parcels of environmental undiluted air, of large dimensions (up to 500 (*m*)) have been observed at all levels in the cloud.

This is the situation that we have in mind when we consider the possible downdraft of environmental air not yet mixed with cloud air. A parcel of environmental air can be pushed to descent by the request of mass and momentum conservation, to compensate the rise of streams of rising cloud air, in a structure of the broken column characterized by coexistence of buoyancy-driven ascent and vertical channels of environmental air. We therefore note that the latter may be not yet cooled by the evaporation of the water after mixing with cloud air close to the top.

Therefore we propose to include in the physical picture the downdraft of pure environmental air, not yet mixed with the cloud air, resulting from the constraints of mass and momentum conservation. The downdrafts are located inside the broken cloud column. In addition, after mixing, the new downdraft will be cooled by evaporation and the mixed parcel will descent even more, up to the cloud base.

During the rise there is a smooth change from the situation of strong stream, specific to the initial stages and the soft slowing down, characteristic of the phase where the column reaches the highest level. In the first phase the contact between the convective column and the environment takes place at the top, at the interface with non-mixed downdraft and at the periphery and in the last phase there is less momentum transfer and easier mutual interpenetration of parcels of air. The exchange of heat and water is less efficient in the first phase and is highly efficient in the last phase, which actually accelerates the process of loss

of buoyancy.

This approximative and descriptive picture suggests to treat separately the two situations. In the first one, the exchanges between the convective column and the environment require to examine the periphery. Close to the final slowing down of the ascending column, the exchanges involve a large volume where parcels of similar dimension of cloud and environmental air are intermingled. Since the top of the column has been in contact with the environment all along the rise, one must represent the breakup of the rising column into smaller columns and the presence, between them, of columns belonging to the initially static environment or downdrafts resulting from evaporative cooling of parcels of mixed air.

These two situations will be our subject. For the problem of cloud periphery, we will discuss the possible evolutions of the interface between the expanding gas and the surrounding air: the shape of the interface, generated the fingering instability and random fluctuations. As expanding front, we examine the formation of *cusp* singularities.

For the problem of breaking of the rising column, we will discuss the statistics of phase competition. We find that, in this schematic representation, based essentially on geometric aspects of competition of two distinct phases of the same gas, it is relevant to discuss in terms of *labyrinth* structured in the horizontal plane.

Therefore we have simultaneously a problem of separation of phases and a problem of interface dynamics. For tractability we divide the problem into two different components: the interface dynamics for each component, as well as for the large boundary circumscribing the full horizontal section of the convective column, is investigated with methods of pole dynamics and/or wrinkled advancing fronts; the phase separation is treated with method of coupled lattice maps, in order to follow easily the breaking of the compact raising column; and, separately.

II. GEOMETRY OF THE INTERFACE BETWEEN THE RISING COLUMN AND THE ENVIRONMENT

A. The exterior interface

1. *Introduction*

It is considered that the the circumference of the cloud at a fixed altitude z has an important role in the exchange of heat and water vapors with the environment. The turbulent diffusion sustained by random eddy exchanges introduces environmental air into the mass of the cloud and there the exchange of heat / vapor modifies the tendency of the column to rise. During the phase of rise the edge of the convective column has a vertical motion relative to the static environment, which creates a layer of vorticity at the interface. There are two mechanisms that can affect this interface, depending on the relative velocity and viscosity. The Kelvin-Helmholtz instability can get a positive growth and peripheric elements of rising column are rolled up to create the known “cats-eye” pattern in a vertical-plane section, *i.e.* a ring vortex with vertical principal axis. Alternatively, a combined lateral expansion and rise of the column can produce the ring vortex at the head of the column, *i.e.* due to the inertial resistance of the static environment, a typical moshroom head (well known from Rayleigh - Taylor instability). In both cases parcels of environmental air are absorbed and entrained being surrounded by cloudy air, thus facilitating the mixing¹³.

If at the circumference the transport processes associated with the entrainment depend on the area of contact between the cloud and the environment then a careful representation of this area is necessary. Equivalently, at fixed altitude z , a good representation of the geometry of the interface cloud/environment is necessary. We will discuss small scale and respectively large scale structure. The small scale structure of the interface is generated by two processes: (1) deterministic instabilities, like *fingering*; (2) random perturbation, related to the turbulence. On a large scale, the structure of the interface can lead the cloud to incorporate (swallow) parcels of environmental air. The mechanism originates in - and is a limiting form of, - the *cusp* singularity that is formed as an asymptotic organization of the small scale quasi-discontinuities.

2. *The small scale structure: the “fingering” instability of the interface*

The interface between the air of a rising column and the environment air shows a specific profile. In every horizontal plane there is a fluid (cloud air) expanding into a static fluid (the environment). An universal model for such process assumes that the velocity of the interface is derived from the gradient of a scalar function that verifies the Laplace equation (is harmonic function). Then the interface is subject to “*fingering*” instability. The role of the Laplacian field is played by the pressure of the expanding gas. We need an analytical instrument to describe the small scale breaking of the continuity of the derivative of the line of the interface. This wiggled profile is the place where the exchange of heat and water vapor takes place.

The two fluids (cloud and external environment) are assimilated with two different phases separated by a moving interface $\Gamma(t)$, a curve in the physical plane of coordinates $[X(t), Y(t)]$. In a simplified representation, the interface is a line that extends between $-\infty$ and $+\infty$, *i.e.* it separates two regions of the plane. The region I is the inside of the cloud, limited by $\Gamma(t)$ and the region II is outside, the environment. It is assumed that the velocity of the expanding fluid (the cloud) is the gradient of a scalar function $P(X, Y)$.

$$\mathbf{v}_n = -(\nabla P)_n \quad \text{at the interface } \Gamma \quad (1)$$

The subscript n means projection of the vector ∇P on the normal at the interface Γ . The equation for the scalar function is 2D Laplace: $\Delta P = 0$ in the cloud region, *i.e.* in the lower part limited by $\Gamma(t)$. This function is $P = 0$ in the free (environment) region II. The physical source of expansion is the input of cloud air from below the current position of the interface $\Gamma(t)$. This is represented as an asymptotic condition for velocity: somewhere very far inside the cloud ($Y \rightarrow -\infty$), the velocity of the air is a constant directed toward the interface

$$\nabla P = \hat{\mathbf{e}}_Y \quad \text{for } Y \rightarrow -\infty \quad (2)$$

In addition

$$P = 0 \quad \text{at the interface } \Gamma \quad (3)$$

3. *The time-dependent complex conformal transformation*

The evolution consists of changes in time of the curve $\Gamma(t) \equiv [X(t), Y(t)]$ representing the interface, *i.e.* expansion of the boundary cloud/environment in any horizontal section of the cloud. The idea is to find a mapping between the physical plane (X, Y) and the complex plane $z \equiv x + iy$. At every moment of time t , the lower semi-plane in the mathematical complex plane (x, y) is mapped to the space below the interface $\Gamma(t)$, where P verifies the Laplace equation. The evolution of the interface is then a set of conformal transformations parametrized by time¹⁴. The scalar function P , is defined as the real part of a new complex variable, whose imaginary part is a function $\Psi(Z)$

$$W(Z) = P(Z) + i\Psi(Z) \quad (4)$$

The two real functions Ψ and P are harmonically conjugated where W is holomorphic.

The conformal map is the function f , $f : \mathbf{C} \rightarrow \mathbf{C}$, $Z \equiv X + iY = f(z, t)$ where $z = x + iy$. Since $f(z, t)$ maps the lower half complex plane ($y < 0$) to the region under $\Gamma(t)$, $Y < 0$, its derivative $\frac{\partial f}{\partial z}$ should have no singularities or zeros in the lower semi-plane. All of them must be in the upper semi-plane. Translating Eq.(2) it is expected that at very large distances on the plane, relative to the interface, the variables will have very close values

$$f(z, t) \sim z \text{ for } z \rightarrow x - i\infty \quad (5)$$

which corresponds to constant velocity of the incoming air, the source being the air rising from below the horizontal plane of the current height.

Now the system is rewritten: the new function (instead of the pressure) is $W(z)$ and the new variables (instead of (x, y)) are z and \bar{z} .

$$\begin{aligned} \frac{\partial W}{\partial \bar{z}} &= 0 \quad (W \text{ is holomorphic}) \\ \frac{\partial W}{\partial z} &= -i \text{ for } z \rightarrow -i\infty \text{ at large distance from } \Gamma \\ \mathbf{Re}W &= 0 \text{ at } z = x - i0 \text{ (at the mapped interface)} \end{aligned} \quad (6)$$

From Eq.(1)

$$\mathbf{Re} \left[\bar{n} \left(\frac{\partial f}{\partial t} + \frac{\overline{\left(\frac{\partial W}{\partial z} \right)}}{\left(\frac{\partial f}{\partial z} \right)} \right) \right] = 0 \quad (7)$$

here \bar{n} is a complex number associated to the normal versor at the interface. The solution is

$$\begin{aligned} W(z) &= -iz \\ &= -if^{-1}(Z, t) \end{aligned} \quad (8)$$

from where the scalar function P is

$$P(X, Y) = \mathbf{Im} [f^{-1}(X + iY, t)] \quad (9)$$

The normal at the interface is

$$\bar{n} = -i \frac{\frac{\partial f}{\partial z}}{\left| \frac{\partial f}{\partial z} \right|} \quad \text{at } z = x - i0 \quad (10)$$

Then the equation describing the *Laplacian growth* is

$$\mathbf{Im} \left(\frac{\partial f(z, t)}{\partial z} \overline{\frac{\partial f(z, t)}{\partial t}} \right) = 1 \quad \text{at } z = x - i0 \quad (11)$$

(for z on the real x axis, just below)

which is the ‘‘Polubarinova - Galin’’ equation^{23, 8, 27, 20, 14, 17}.

A particular form of the solution f is derived by Ponce Dawson and Mineev Weinstein in Refs.^{23, 8, 27}. Since f is holomorphic in the lower complex half-plane a general expression is defined by choosing for $\frac{\partial f}{\partial z}$ a number of zeros and poles in the upper half-plane. This provides the explicit form of the mapping, at a fixed moment of time. Since we have assumed infinite extension of the interface, a class of solutions is

$$f_{\text{inf}}(z, t) = z - it - i \sum_{l=1}^{N+1} \alpha_l \log [z - \zeta_l(t)] \quad (12)$$

where

$$\alpha_l \equiv \alpha'_l + i\alpha''_l \quad \text{are } N + 1 \quad \text{complex constants} \quad (13)$$

and (α', α'') are real.

$$\zeta_l \equiv \xi_l + i\eta_l \quad \text{are } N + 1 \quad \text{singularities} \quad (14)$$

simple poles of $\frac{\partial f}{\partial z}$ that move in time.

A detailed treatment of the conformal mapping is provided in the Appendix A. The evolution keeps the zeros and the poles in the upper half-plane, where they are initialized. At any moment of time the new positions of the singularities are inserted in Eq.(12) and the conformal mapping is determined. Therefore we have the new shape of the interface between the two physical media (expanding cloud and environment).

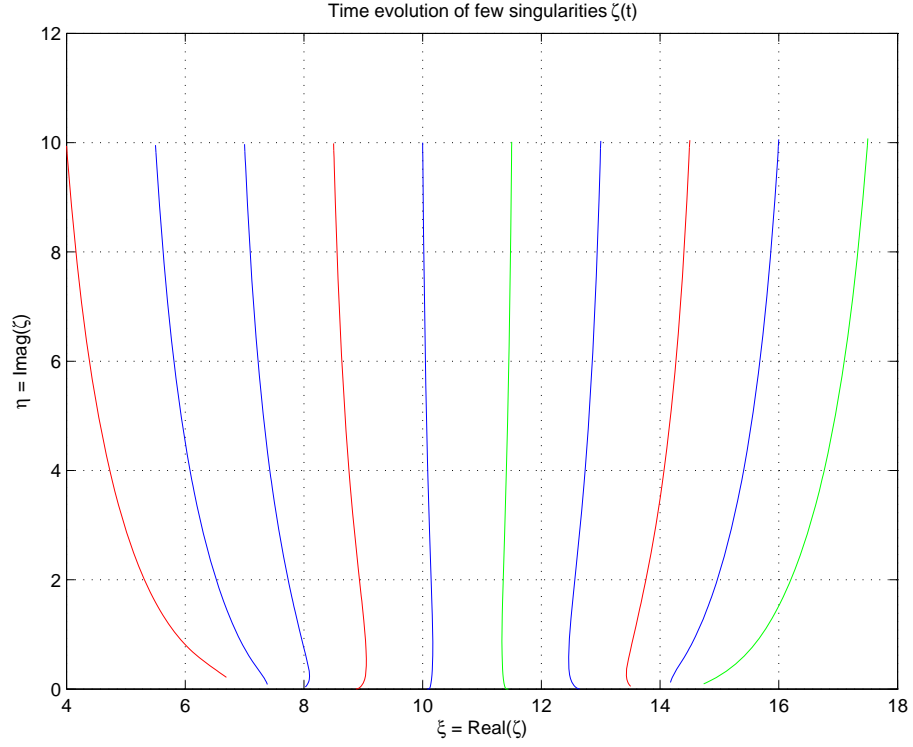


Figure 1: The curves represent the time evolution of the positions of the $N + 1$ singularities $\zeta_k(t) = [\xi_k(t), \eta_k(t)]$, ($k = 1, N + 1$ for $N = 9$). The initial positions $\eta_k(t = 0)$ are at in a small interval around 10 and the real parts $\xi_k(t = 0)$ are distributed on equal intervals.

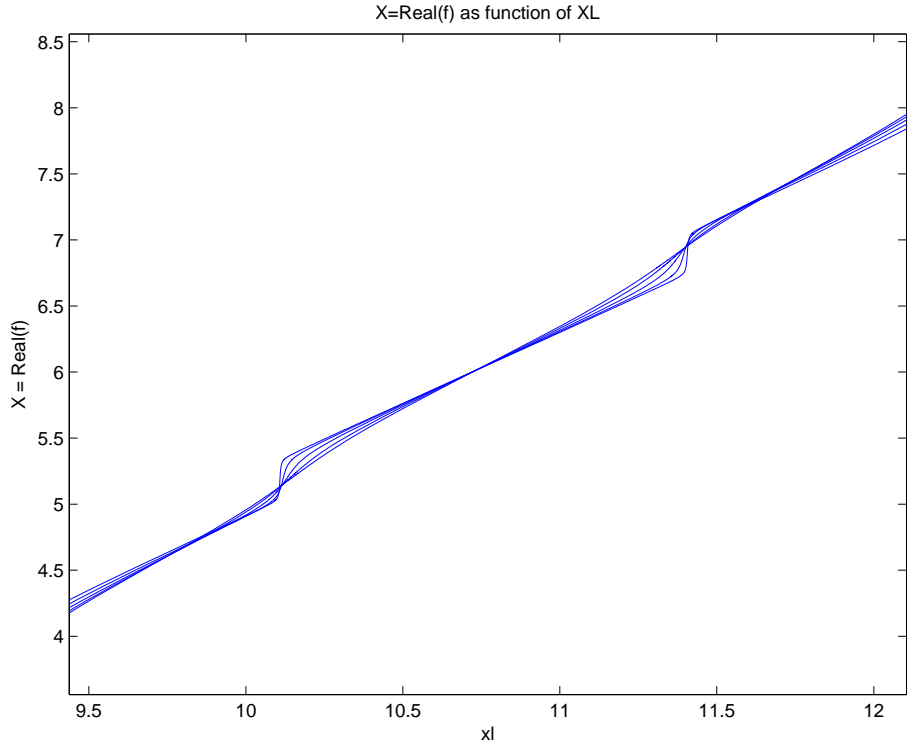


Figure 2: The lines $X(t) \equiv \mathbf{Re}[f(z, t)]$ at 5 moments of time, $t = 90, \dots, 95$. Since both real and imaginary parts of ζ_l are not too close to 0, the lines are smooth.

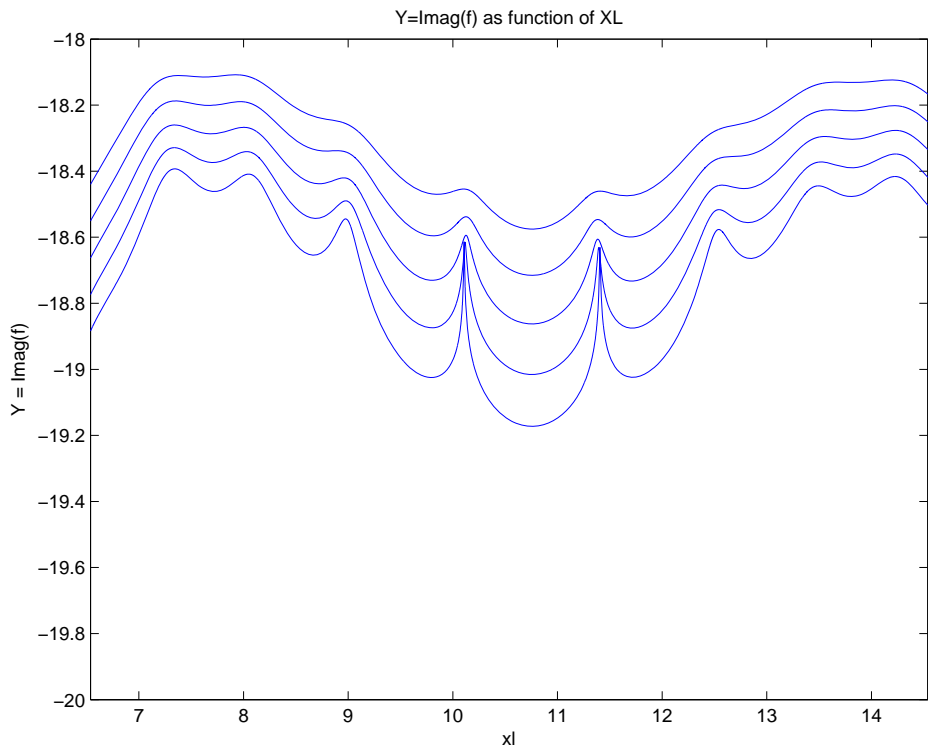


Figure 3: Same as Fig2 for $Y(t) \equiv \mathbf{Im}[f(z, t)]$.

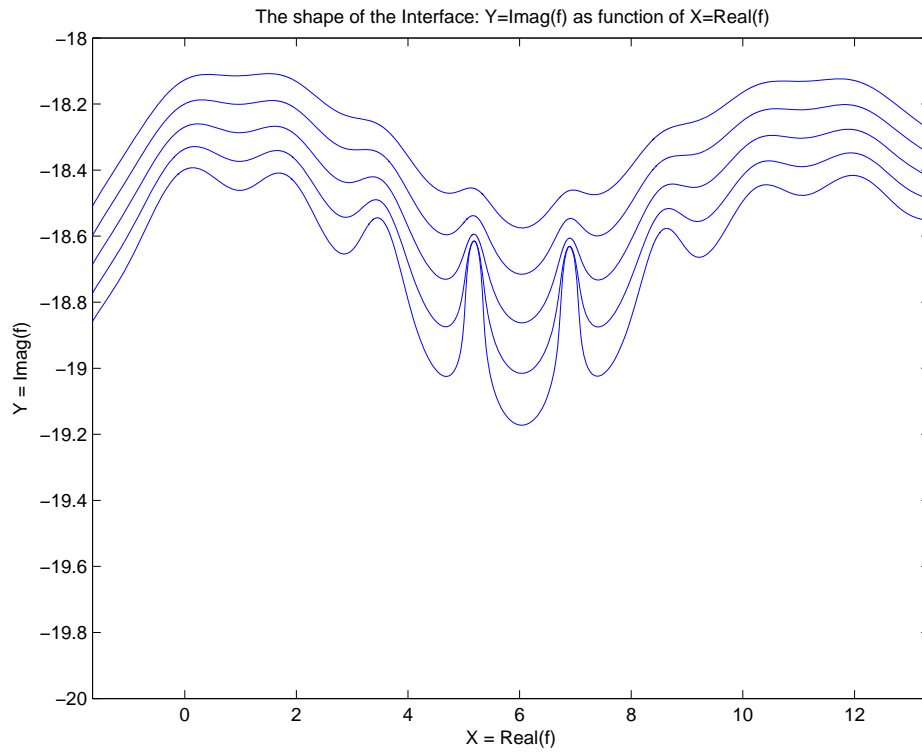


Figure 4: The interface at 5 moments of time, as in Figs2 and 3.

B. The small scale structure: roughening of the interface due to random fluctuations

Besides the deterministic evolution described by the *fingering* instability, one should consider random fluctuations that produces the roughening of the interface. It has been found that the interface roughness in $2D$ is algebraic on short length scale. Here we only mention from Ref.¹⁸ a part of the argument that introduces the Hilbert transform. This is an analytical step which prepares the discussion on the large scale features of the cloud boundary. We consider the interface between the cloud and the environment consisting, in the horizontal plane, of a line Γ of length L . The coordinate along the interface is s and along the local normal is y . The position in plane of the current point on the interface is given by the distance

$$h(s, t)$$

relative to a fixed reference system. The Laplacian field (the pressure) $\phi(\mathbf{x}, t)$ is defined as

$$\begin{aligned} \Delta\phi &= 0 \quad \text{for } y < h \quad \text{inside the cloud, and} \\ \phi &= 0 \quad \text{for } y > h \end{aligned} \tag{15}$$

The velocity of a current point of the interface is given by the *gradient of the scalar function* ϕ , as

$$\frac{\partial h}{\partial t} = -D \left(\frac{\partial\phi}{\partial y} - \frac{\partial\phi}{\partial s} \frac{\partial h}{\partial s} \right)_{x=h} \tag{16}$$

This equation describes the *gradient flow*. The last term describes the local dilation or the compression of the length of the curve Γ . The deterministic part of the dynamics is introduced by the average motion of the front

$$h = Vt \tag{17}$$

A small perturbation of the “height” $h(x, t)$ taken as

$$\tilde{h}_q(s) = h_q(t) \exp(iqs) \tag{18}$$

acting on the moving interface decays as

$$\left| \tilde{h}_q(s) \right| \sim \exp[-\sigma(q)t] \tag{19}$$

so the perturbation is exponentially vanishing with the rate

$$\sigma(q) = V |q| \quad (20)$$

Then the relaxation of the interface “height” is a simple linear decay of the logarithm of h_q , working in the Fourier space. Since we want to take into account the random fluctuations, it is introduced a noise source

$$\frac{\partial h_q(t)}{\partial t} = -V |q| h_q(t) + \eta_q(t) \quad (21)$$

This is a nonlocal equation since $\sigma(q)$ acts in Fourier space. The noise is Gaussian

$$\langle \eta_q(t) \eta_{q'}(t') \rangle = \frac{\Delta}{L} \delta(q + q') \delta(t - t') \quad (22)$$

We note that the dynamical equation for the noise-driven interface contains the term $-V |q| h_q(t)$. It comes from taking the Fourier transform of the real-space function h , multiplying with the absolute value of the Fourier space variable $|q|$ and returning to real space. This is the Hilbert transformation applied on h and will play an essential role in the following.

In Ref.¹⁸ it is shown that the width of the interface increases as the \log of the length L .

C. The large scale dynamical structuring of the interface: cusp singularities

We are now interested in the phase of the cloud expansion where the convection flux coming from lower levels is progressively reduced, the column reaching a regime of quasi-stationarity. On a large spatial scale (of the circumference of the expanding cloud) the interface has a dynamics of the expansion of a front as the propagation of a planar flame into a static homogeneous medium. A model equation for the latter case has been developed by Sivashinsky^{30,22}. It treats the advancement of a front of a flame in a channel.

The planar flames expanding freely has an interface that is unstable. For a simple model in $1D$ (flames propagating in a channel of width \tilde{L}) the variable is

$$h(x, t) \equiv \text{position of the flame front above the } x \text{ axis}$$

The equation of Sivashinsky³⁰ is

$$\frac{\partial h(x, t)}{\partial t} - \frac{1}{2} \left[\frac{\partial h(x, t)}{\partial x} \right]^2 - \Lambda \{h(x, t)\} = \nu \frac{\partial^2 h(x, t)}{\partial x^2} + 1 \quad (23)$$

in the domain

$$0 < x < \tilde{L}$$

The functional Λ is the Hilbert transform. To define its action, first one makes the Fourier transform of the function $h(x, t)$,

$$h(x, t) = \int_{-\infty}^{\infty} \exp(ikx) \hat{h}(k, t) dk \quad (24)$$

then multiply $\hat{h}(k, t)$ by the absolute value of the Fourier variable

$$\Lambda \{h(k, t)\} = |k| \hat{h}(k, t) \quad (25)$$

and returns to the real space, $\Lambda \{h(x, t)\}$. We can trace the occurrence of the Hilbert operator in the equation for the front advancement from the derivation of Eq.(21).

The front is unstable and it generates singularities in finite time. The singularities are of the *cusp* type. We note that this evolution implicitly renders the interface piecewise smoother since it collects the smaller scale singularities into a single, *giant cusp*. This corresponds to the late phases, where the flux of cloud air is reduced and the reserve of buoyancy is decaying.

1. *Formalism: Pole decomposition*

The origin of the *cusp* profile can be understood from the evolution of the positions of the complex singularities (poles) of the solution. The motion of the pole singularities is controlled by the Hilbert operator. The multiplication with the absolute value of the Fourier variable $|k|$ is equivalent to the differential operator $i \frac{\partial}{\partial x}$. It makes the poles to approach the real axis, from both sides. The accumulation of poles (“condensation” at the limit of continuous density of poles) leads to the formation of the *cusp*, a singularity of the interface that is qualitatively similar with what is frequently seen in the evolution of an expanding cloud. This suggests that the large scale structure at the expansion of the circumference of a cloud as it rises can be studied using the Sivashinsky equation, (23).

Therefore the first step in an analytic development is to extend the space coordinates to complex variables^{20, 14, 1, 5, 16, 15}. The nature of processes that take place during time evolution is: (1) attraction between the poles along the horizontal axis (x or θ) leading to clusterization

of poles along vertical direction in the complex plane, and (2) dynamical evolution of the poles towards the real axis. This produces singularities that look like *cusps*.

The problem is restricted to a single space variable, relative to which we measure the spatial position $h(x, t)$ of the interface. The nature and the positions of the wrinkles of the interface can be associated to the singularities of the interface - function in the plane of the complexified spatial variable. A singular profile will occur in finite time but for short time the equation is integrable which means that it has the Painleve property and the formal solution is meromorphic and can be written as an expansion in a set of order-one poles.

In Ref.³² it is proposed the Lagrangian version of Eq.(21) with the white noise converted into a diffusion generated by viscosity ν , essentially constructed on the ground of Burgers equation

$$\frac{\partial u}{\partial t} + u \frac{\partial u}{\partial x} = \Lambda[u] + \nu \frac{\partial^2 u}{\partial x^2} \quad (26)$$

As before, $\Lambda[u] : \hat{u}(k, t) \rightarrow |k| \hat{u}(k, t)$ where the Fourier transform of the function u has been introduced $u(x, t) = \int_{-\infty}^{+\infty} dk \exp(ikx) \hat{u}(k, t)$. The solution is a meromorphic function expressed in terms of simple poles by terms like

$$p_\alpha = \frac{1}{x - z_\alpha} \quad (27)$$

The operator Λ applied on such term results in

$$\begin{aligned} \Lambda p_\alpha &= \Lambda \left[\frac{1}{x - z_\alpha} \right] \\ &= \text{sign}[\text{Im}(z_\alpha)] i \frac{\partial}{\partial x} p_\alpha(x) \end{aligned} \quad (28)$$

The operator Λ produces advection of the poles, along the imaginary direction, towards the real axis (both from above and from below since the operator multiplies with $|k|$). This enhances the effect of the singularity, *i.e.* the real function which is the solution becomes even more perturbed there. The typical profiles are *quasicusps*, which are cusps with the tip rounded due to the presence of ν . In Refs.^{32,10} this is explained by showing that the singularities never reach the real axis, but remains at a distance whose expression is given by ν . This will produce *wrinkles*. The *solution* of the Eq.(26) can be written, for the linear geometry as

$$u(t, x) = -2\nu \sum_{\alpha=1}^{2N} \frac{1}{x - z_\alpha(t)} \quad (29)$$

where $z_\alpha(t)$ are $2N$ poles placed symmetrically, as complex conjugated pairs ($u(x, t)$ results *real*) relative to the real axis. The equations of motion is

$$\frac{dz_\alpha}{dt} = -2\nu \sum_{\beta \neq \alpha} \frac{1}{z_\alpha - z_\beta} - i \text{sign} [\text{Im}(z_\alpha)] \quad (30)$$

The poles tend to attract themselves *horizontally*, parallel with the real axis. As noted in Ref.²⁴ this results from the dominant behavior of the x coordinate of the poles

$$\frac{dx_j}{dt} \sim - \sum_{k \neq j} \sin(x_j - x_k) [\dots]$$

In the paranthesis [...] there are terms that are invariant to the change $x_j \leftrightarrow x_k$, for any pair $j, k = 1, N$, with $j \neq k$. This factor is positive. When $0 < x_j < x_k$ we have $dx_j/dt > 0$ and for $0 < x_k < x_j$ we have $dx_j/dt < 0$. In both cases, x_j evolves to be closer to x_k .

In addition there is a tendency of the poles to place themselves on a line parallel to the imaginary axis (this is the analog of the same phenomenon for the Burgers equation). At short range the poles tend to repel each other vertically and the repulsion between two poles aligned on a vertical (y) line becomes infinite when they come too close. At longer distances, the interaction become attractive.

Details on the integration of Eq.(30) are in Appendix B.

2. *Further developments*

The stability of the interface consisting of a giant cusp has been examined in²⁴ and¹⁹ where it is explained the role of the noise in generation of new poles in the structure of the solution. This may also explain the self-fractalization of the interface resulting from self-acceleration⁹ of the flame front determined experimentally¹².

III. THE BREAKING OF THE RISING CONVECTION COLUMN

A. Introduction. The loss of compacity of the column

During its rise the convective column may undergo breakup and loss of compacity in its volume. The column will then consist of vertical streams of cloudy air separated by volumes of environmental air, also vertical and of irregular shape, which is either static and not yet

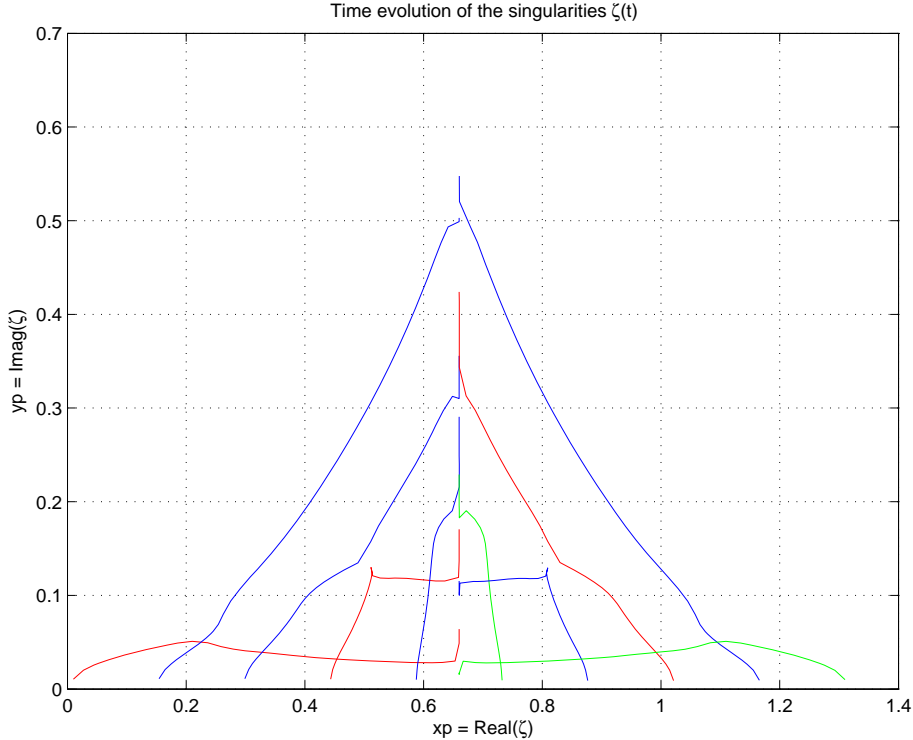


Figure 5: The time evolution of the complex poles of the solution of the interface problem for the case of the *cusp* singularity.

mixed or consists of downdrafts after evaporative cooling of parcels entrained close to the top of the column. As recalled in the Introduction, the simplest view on the convection is a picture of interpenetration of two gases, one being the stream of rising air whose ascension is sustained by buoyancy and the other being the environment. There is a wide spectrum of possible evolutions, from the early loss of the streaming compacity to the preservation of robust columnar features during all rise. We try to find an analytical representation of the breaking of the rising column.

There are observations revealing that, on a horizontal plane, the updraft inside a cloud presents substantial inhomogeneity^{31, 26, 21}. There are large variations of the vertical velocity, in magnitude and sign, meaning that there are updrafts and downdrafts and also regions of static environmental air. It results that there is a breaking-up of the rising column. Obviously, the surface of contact between the convective air and the environment, either static or penetrative downdrafts, is much larger than in the case where the column remained compact as it rises. The examination of the breaking up of the column, with substantial increase of the “interface”, is a necessary step in a better representation of the exchanges

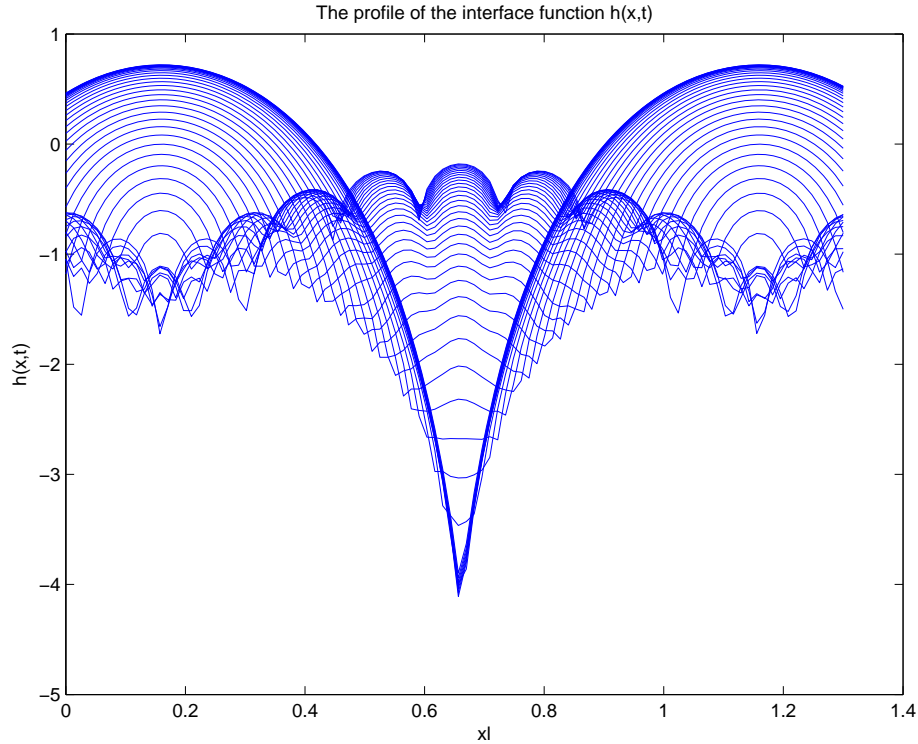


Figure 6: The profile of the interface at several moments of time. The initial state has many oscillations of small amplitude and the final state presents the cusp singularity.

and transport processes. In particular this refers to the model of Squires³¹ where it is assumed that the environmental air is mixed with the cloud at the cloud top. Then, due to evaporative cooling, the mixed air loses its buoyancy and descends deep into the cloud column (kilometers)²⁶. The exchange of heat and vapors with the cloud air continues for these *internal* downdrafts and the result is dilution of the cloud air but also increase of the buoyancy of the air penetrating from above. The equilibrium between the penetrating downdrafts and the cloud air surrounding it is reached at equal buoyancy.

We are interested in the process of competition between the rising air of the convective column and the environmental air. The result is the physical breakup of the column and the coexistence, at every horizontal level, of regions of rising air and of environmental air. The inhomogeneity of the cloud can be pronounced: inside the clouds there are narrow updraft regions but between them there are strong negative vertical velocity flows, due to rapid downdrafts²¹. This pattern, in the horizontal plane, justifies the use of a model of interface dynamics which exhibits the *labyrinth* instability.

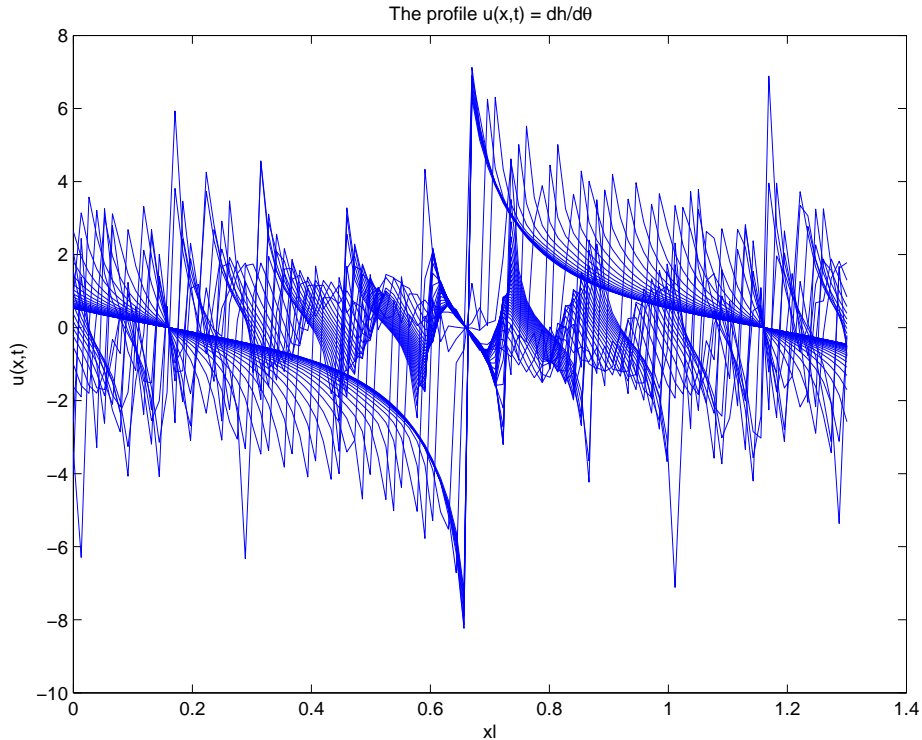


Figure 7: The slope of the interface.

B. The breaking of the convective column as a phase-competition dynamics

We look for a schematic analytical and/or numerical description to the real phenomenon of breaking of the rising column into distinct vertical streams separated by regions of environmental air. It is easier to restrict to horizontal planes. The most elementary representation consists of the separation of phases of a fluid in $2D$. For a binary fluid the variable is the concentration c where the two pure phases have $c = \pm 1$. The dynamics is described by a parabolic equation where the local change of the concentration is the Laplacian flow of the density of a functional of c , which can be called “chemical potential”. The free energy decays to zero when there is full separation of phases, *i.e.* the two phases occupy disjoint regions in plane. These regions can look similar to a *labyrinth* pattern¹¹. For example, in the final stage of the slowing down of the rise of the cloud, where substantial loss of buoyancy has resulted from mixing with environment, the horizontal plane is mostly covered by regions of environmental air, with few patches of cloud.

Technically, we can use the analytical approach based on one of the standard models, in particular Cahn-Hilliard system, studied in Ref.¹¹, or cellular automata³. However it is more useful to implement another aspect besides the phase-separation: phase competition.

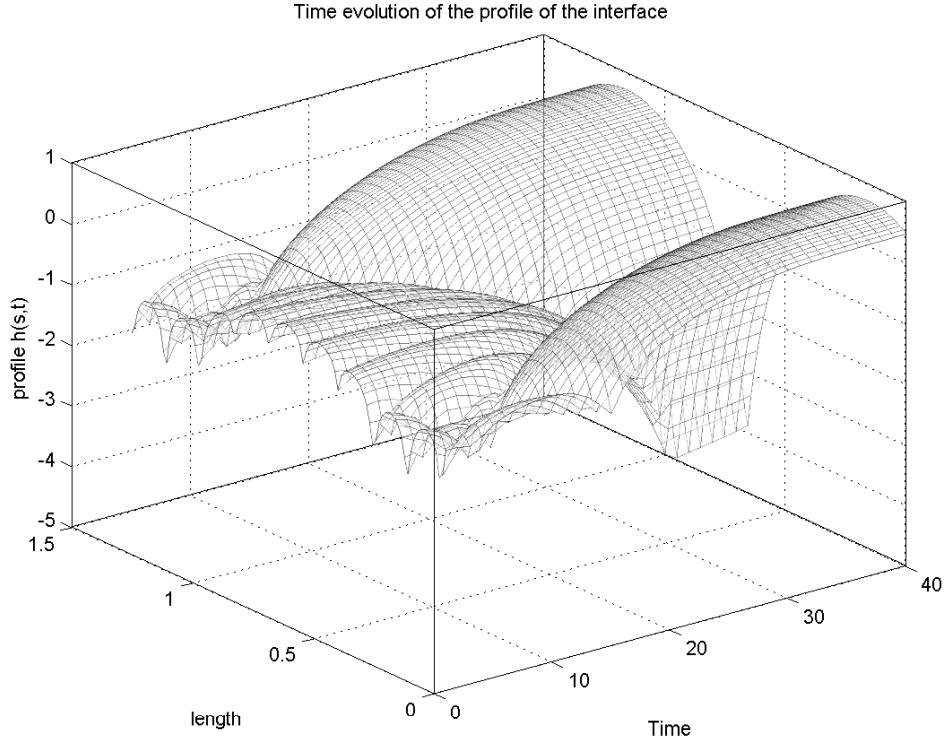


Figure 8: The relief view of the evolution of the interface.

In similar cases it has been adopted a representation of dynamical phase transition which employs a system of coupled cubic map lattice²⁵.

If the two phases have the same stability then the motion of the interface is governed as in a gradient flow, by the local curvature. If the two phases have distinct stability properties then the most stable phase will advance irreversibly into the other and will eventually replace it. The problem belongs to the same class as phase separation and nucleation phenomena.

The coupled lattice maps are described by the set of equations for a discretized variable $q(\mathbf{x}, t)$ which represents the nonconserving order parameter at the points of a regular lattice

$$q(\mathbf{i}, t + 1) = f[q(\mathbf{i}, t)] + \gamma \left[\sum_{\mathbf{j}=n.n}^p q(\mathbf{j}, t) - pq(\mathbf{i}, t) \right] \quad (31)$$

where $\mathbf{i} \equiv (i_1, i_2, \dots)$ is a set of integers that specifies the position of a point in the lattice. In our case the dimension of the problem is $d = 2$ (plane), $\mathbf{i} \equiv (i_1, i_2) = (i_x, i_y)$. The sum in the square paranthesis extends over the *nearest neighbors* (*n.n*) of the point \mathbf{i} of the lattice. They are in number of p in general and in $d = 2$ they are $p = 4$. The square paranthesis is actually a discretization of the Laplace operator and this term represents the diffusion.

The nonlinearity of the dynamics of the order parameter $q(\mathbf{x}, t)$ is introduced by the term

$$f[q(\mathbf{i}, t)] = -q^3 + (1 + \varepsilon)q + c \quad (32)$$

We recognize easily the meaning of choosing this nonlinearity. The “potential” f has two extrema, corresponding to non-dynamical equilibria. The order parameter can take one or another of these two equilibria values, and they are associated to the two states. The dynamical equation for $q(\mathbf{x}, t)$ is a discretized form of the Landau-Ginzburg equation.

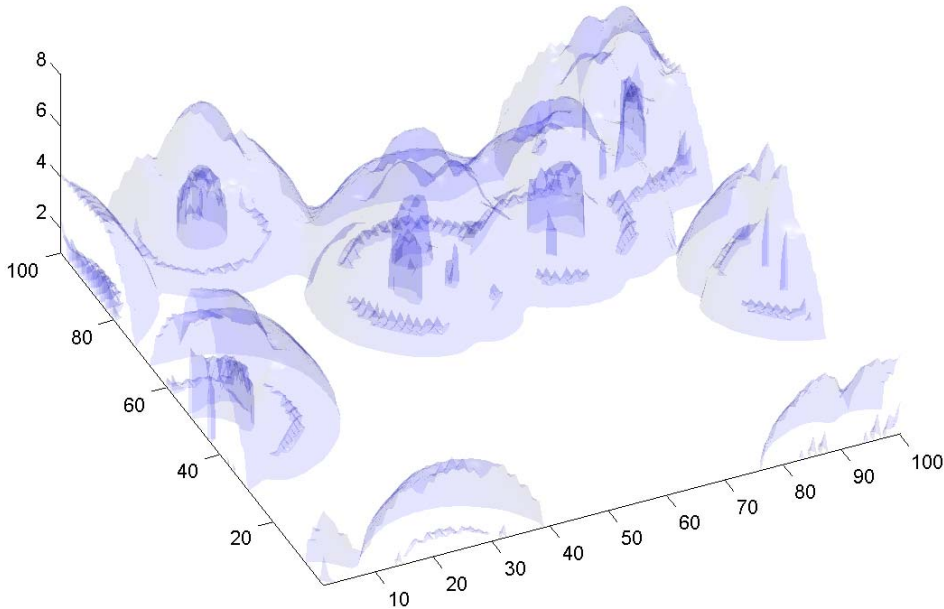


Figure 9: The end stage of the competition between two phases (which we would attribute to cloud, respectively environment). The vertical axis is the height of successive planes that are labelled by the time in the iterative map Eq.(31). The parameters are $a = 1$, $\varepsilon = 0.65$, $c = 0.10$ and $\gamma = 0.09$.

C. Phase separation for equally stable states

This corresponds to

$$c = 0 \quad (33)$$

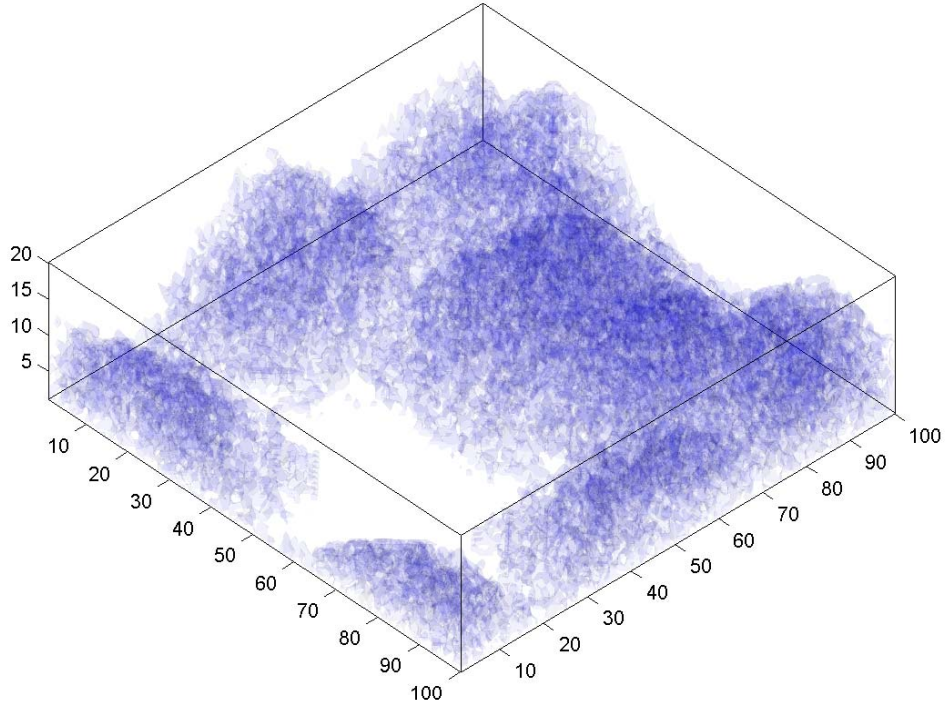


Figure 10: The same as Fig.9, for $a = 1$, $\epsilon = 0.45$, $c = 0.6$ and $\gamma = 0.06$.

and the initial state is

$$q_0(i, j) = 0 \quad (\text{stable}) \quad (34)$$

$$+\xi \quad (\text{zgomot})$$

The spatial competition produces clusters of one phase inside the other. Any curved frontier between the two phases evolves with a velocity²⁵

$$v = -\gamma K \quad (35)$$

transversal on the boundary. K is the curvature of the boundary. For a disk of radius R the curvature $K = R^{-1}$ and the evolution is symmetrical with

$$R^2(t) - R^2(0) = -2\gamma t \quad (36)$$

The initial situation is a compact covering of the domain of interest with a single phase. This initial state is perturbed by the random nucleation of the other phase on small regions. The evolution consists of extension of the regions associated with the Phase II, against the Phase I and the break up of the region initially occupied by only the Phase I. The process

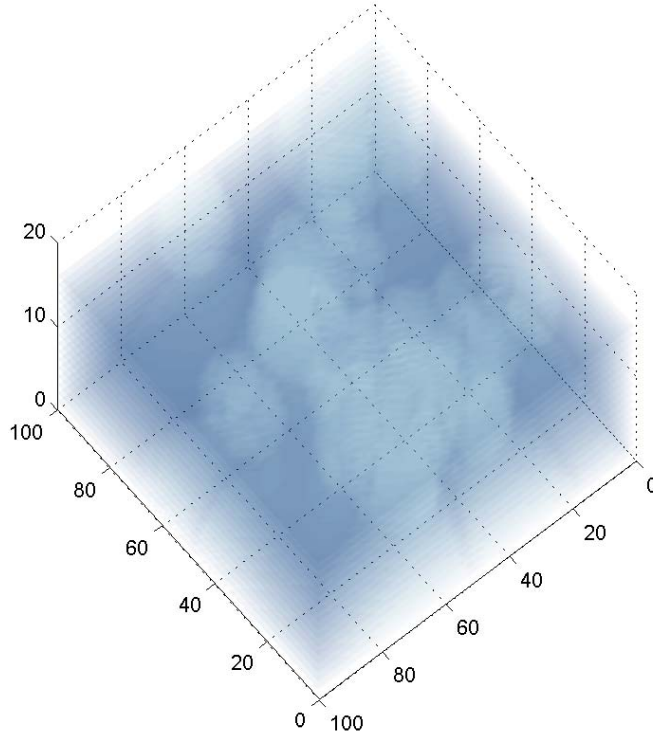


Figure 11: The competition of the two phases is shown as results from iteration. The structure (barely visible) has the small scale oscillations related to the propagation mode at the level of one mesh cell length.

leads to the loss of compacity of the region of Phase I (cloud) and to progressive reduction of the surface occupied by it in horizontal planes.

It has been proved²⁵ that the iterative update adopted in Eq.(31) and (32) is equivalent with the curvature flow Eq.(35). The dynamic structure function, defined as the discrete Fourier transform of the correlation of the field $q(i, j, t)$ has at large time a decay like $t^{1/2}$. We note however that this is a purely geometric property, and the cloud-environment mixing is not taken into account. We have however a lower bound to the rate of disappearance of compact parcels of cloud in the late phases of the convection.

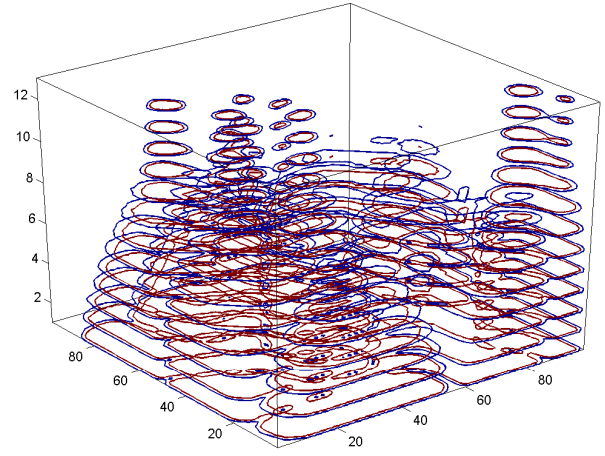
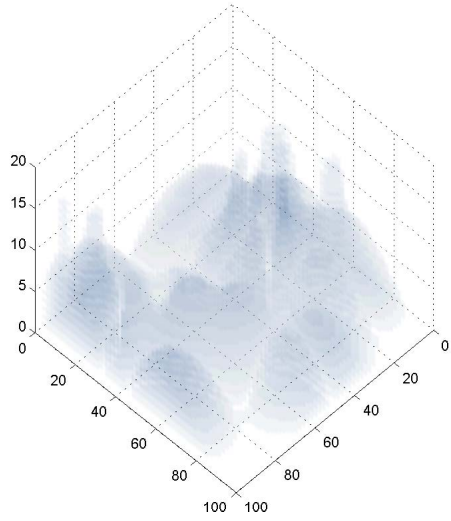
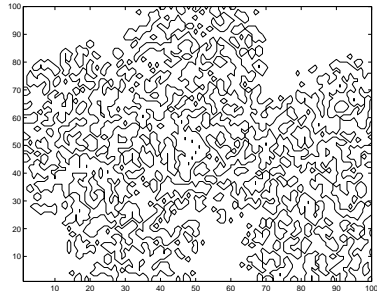
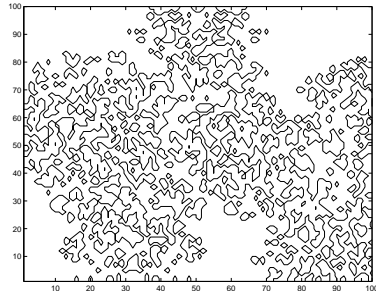


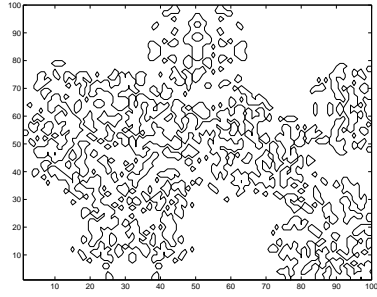
Figure 12: Left: Same as Fig.11 after artificially removing the small scale oscillation. This makes more visible the two phases. Right: The contour slices of the left figure, that are used for calculation of the length of the circumference of horizontal patches.



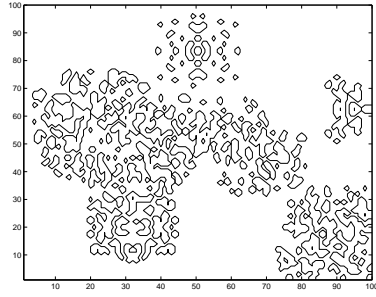
(a)



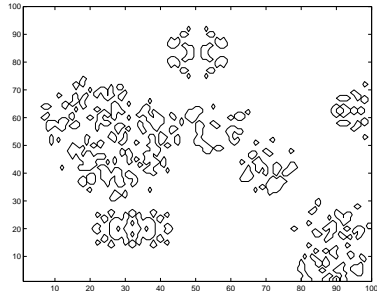
(b)



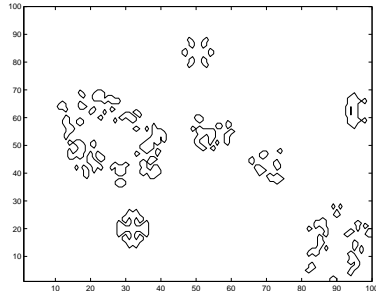
(c)



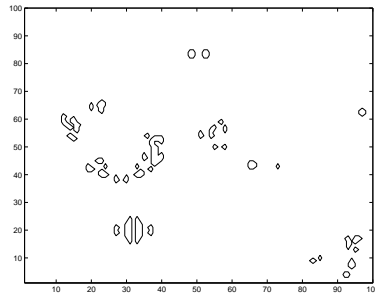
(d)



(e)

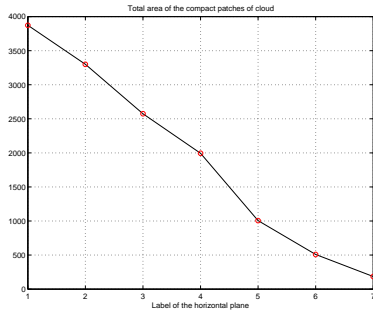


(f)

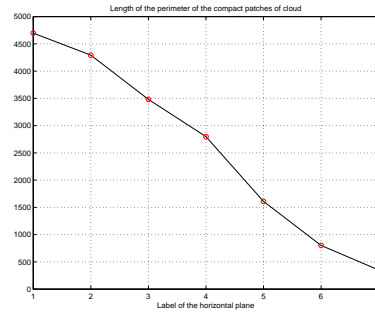


(g)

Figure 13: The contour levels corresponding to patches of compact cloudy air in several horizontal planes.



(a)



(b)

Figure 14: Area and length of the perimeter of compact patches of cloud air, with dependence on the height of the horizontal plane. The latter variable is mapped from the variable time of the iterative sequence. The parameters are: $a = 1$, $\beta = 0.45$, $c = 0.6$, $\gamma = 0.06$ and time step 0.02. The figures correspond to 200 time steps.

IV. CONCLUSIONS

We have examined three geometrical aspects that can be important in the quantitative studies of the exchanges of heat and vapor between the cloud and the environment.

The first model, regarding the *fingering* instability can be an important step in representing the fractalization of the boundary of the clouds.

The second model, intended to allow a quantitative description of the *cusp* singularity of the interface, can be also implemented in any study of the lateral exchanges cloud-environment. It can be developed further for the study of the process of absorption of parcels of environmental air inside the cloud, but this is a problem of complex function with a certain difficulty.

Finally we have considered the possibility to describe the loss of compacity of the rising column by a discrete, coupled lattice map model. At least the basic facts of decay of the convection and loss of continuity of the cloud tower, can be examined using this model.

A wide range of similar models can now be proposed and further development can be considered.

Acknowledgments

This work is partially supported by the Contract PN 09 39 01 01.

A. APPENDIX. THE INTERFACE DEVELOPING FINGERS IN LAPLACIAN GROWTH

A. Interface between infinite regions

The evolution of the front of the expanding cloud, in any horizontal plane, is represented through the conformal mapping from the lower half of the “mathematical plane” on the region below Γ , the interior of the cloud. The *Laplacian growth* is described by the **Polubarinova - Galin** (P-G) equation

$$\mathbf{Im} \left(\frac{\partial f(z, t)}{\partial z} \overline{\frac{\partial f(z, t)}{\partial t}} \right) = 1 \text{ at } z = x - i0 \quad (\text{A.1})$$

(for z just below the real x axis)

A class of solutions is^{23, 8, 27}

$$f_{\text{inf}}(z, t) = z - it - i \sum_{l=1}^{N+1} \alpha_l \log [z - \zeta_l(t)] \quad (\text{A.2})$$

where

$$\alpha_l \equiv \alpha'_l + i\alpha''_l \quad \text{are } N + 1 \quad \text{complex constants} \quad (\text{A.3})$$

and (α', α'') are real.

$$\zeta_l \equiv \xi_l + i\eta_l \quad \text{are } N + 1 \quad \text{singularities} \quad (\text{A.4})$$

simple poles of $\frac{\partial f}{\partial z}$ that move in time.

Let us calculate explicitly

$$\frac{\partial f}{\partial z} = 1 - i \sum_{l=1}^{N+1} \alpha_l \frac{1}{z - \zeta_l(t)} \quad (\text{A.5})$$

and

$$\frac{\partial f}{\partial t} = -i - i \sum_{l=1}^{N+1} \alpha_l \frac{1}{z - \zeta_l(t)} \frac{d\zeta_l(t)}{dt} \quad (\text{A.6})$$

$$\overline{\frac{\partial f}{\partial t}} = i + i \sum_{l=1}^{N+1} \overline{\alpha_l} \frac{1}{\overline{z - \zeta_l(t)}} \frac{d\overline{\zeta_l(t)}}{dt} \quad (\text{A.7})$$

and the product is

$$\begin{aligned} \frac{\partial f}{\partial z} \overline{\frac{\partial f}{\partial t}} &= \left(1 - i \sum_{l=1}^{N+1} \alpha_l \frac{1}{z - \zeta_l(t)} \right) \left(i + i \sum_{l=1}^{N+1} \overline{\alpha_l} \frac{1}{\overline{z - \zeta_l(t)}} \frac{d\overline{\zeta_l(t)}}{dt} \right) \quad (\text{A.8}) \\ &= i \\ &\quad + \sum_{l=1}^{N+1} \alpha_l \frac{1}{z - \zeta_l(t)} \\ &\quad + i \sum_{l=1}^{N+1} \overline{\alpha_l} \frac{1}{\overline{z - \zeta_l(t)}} \frac{d\overline{\zeta_l(t)}}{dt} \\ &\quad + \sum_{l=1}^{N+1} \sum_{k=1}^{N+1} \alpha_l \overline{\alpha_k} \frac{1}{z - \zeta_l(t)} \frac{1}{\overline{z - \zeta_k(t)}} \frac{d\overline{\zeta_k(t)}}{dt} \end{aligned}$$

This must be taken for the line that in the mathematical (complex) plane z represent the interface

$$z \rightarrow x - i0 \quad (\text{A.9})$$

which means that z will be replaced everywhere with real x . Before doing this we make a test, looking at what this expression becomes when we replace

$$z \rightarrow \overline{\zeta_m(t)} \quad (\text{A.10})$$

and find for the first two terms

$$\begin{aligned} & + \sum_{l=1}^{N+1} \alpha_l \frac{1}{z - \zeta_l(t)} + i \sum_{l=1}^{N+1} \overline{\alpha_l} \frac{1}{\overline{z - \zeta_l(t)}} \frac{\overline{d\zeta_l(t)}}{dt} \\ \rightarrow & \sum_{l=1}^{N+1} \alpha_l \frac{1}{\zeta_m(t) - \zeta_l(t)} + i \sum_{l=1}^{N+1} \overline{\alpha_l} \frac{1}{\overline{\zeta_m(t) - \zeta_l(t)}} \frac{\overline{d\zeta_l(t)}}{dt} \end{aligned} \quad (\text{A.11})$$

According to^{8,27} the replacement $z \rightarrow \overline{\zeta_m}$ in the expression of the function f produces *constants* due to the fact that f verifies the equation **Polubarinova Galin**, as will be proved further below. These constants are denoted β_m . After that we take the imaginary part

$$\begin{aligned} & 1 \\ & + \mathbf{Im} \left[\sum_{l=1}^{N+1} \alpha_l \frac{1}{x - \zeta_l(t)} \right. \\ & + i \sum_{l=1}^{N+1} \overline{\alpha_l} \frac{1}{x - \zeta_l(t)} \frac{\overline{d\zeta_l(t)}}{dt} \\ & \left. + \sum_{l=1}^{N+1} \sum_{k=1}^{N+1} \alpha_l \overline{\alpha_k} \frac{1}{x - \zeta_l(t)} \frac{1}{x - \zeta_k(t)} \frac{\overline{d\zeta_k(t)}}{dt} \right] \\ & = 1 \end{aligned} \quad (\text{A.12})$$

B. The constraints resulting from the P-G equation

1. The algebraic system

The invariants of the solutions to the equations P-G are

$$\beta_k = f_k(\overline{\zeta_k}, t) = \overline{\zeta_k} - it - i \sum_{l=1}^{N+1} \alpha_l \log(\overline{\zeta_k} - \zeta_l) \quad (\text{A.13})$$

Here we apply the operator d/dt

$$0 = \frac{d\overline{\zeta_k(t)}}{dt} - i - i \sum_{l=1}^{N+1} \alpha_l \frac{1}{\overline{\zeta_k(t)} - \zeta_l(t)} \left(\frac{d\overline{\zeta_k(t)}}{dt} - \frac{d\zeta_l(t)}{dt} \right) \quad (\text{A.14})$$

Or, write first the real and imaginary parts of the constants β_k . We have

$$\begin{aligned}\log(\bar{\zeta}_k - \zeta_l) &= \log[(\xi_k - \xi_l) + i(-\eta_k - \eta_l)] \\ &= \log(|(\xi_k - \xi_l) - i(\eta_k + \eta_l)|) \\ &\quad + i \arg[(\xi_k - \xi_l) - i(\eta_k + \eta_l)]\end{aligned}\tag{A.15}$$

The modulus is

$$\begin{aligned}\log[|(\xi_k - \xi_l) - i(\eta_k + \eta_l)|] \\ = \frac{1}{2} \log[(\xi_k - \xi_l)^2 + (\eta_k + \eta_l)^2]\end{aligned}\tag{A.16}$$

The phase is

$$\arg[(\xi_k - \xi_l) - i(\eta_k + \eta_l)] = \arctan\left(\frac{\eta_k + \eta_l}{\xi_k - \xi_l}\right)\tag{A.17}$$

When the abscissa $\xi_k - \xi_l$ is negative the complex argument $\bar{\zeta}_k - \zeta_l$ crosses the cut and we have to add $\iota\pi$.

In addition, when two singularities are such that $\bar{\zeta}_k = \zeta_l$ we have

$$\begin{aligned}\bar{\zeta}_k - \zeta_l = 0 &\rightarrow \xi_k - \xi_l = 0 \quad \text{and} \quad \eta_k + \eta_l \rightarrow 2\eta_k \\ \text{we have } \arctan\left(\frac{\eta_k + \eta_l}{\xi_k - \xi_l}\right) &\rightarrow \frac{\pi}{2}\end{aligned}\tag{A.18}$$

Then

$$\begin{aligned}\beta'_k &= \xi_k - \sum_{l \neq k} \alpha'_l \arctan\left(\frac{\eta_k + \eta_l}{\xi_k - \xi_l}\right) \\ &\quad - \frac{1}{2} \pi \alpha'_k - \pi \sum_{l; \xi_k - \xi_l < 0} \alpha'_l + \alpha''_k \log(2\eta_k) \\ &\quad + \frac{1}{2} \sum_{l \neq k} \alpha''_l \log[(\xi_k - \xi_l)^2 + (\eta_k + \eta_l)^2]\end{aligned}\tag{A.19}$$

and for the imaginary part

$$\begin{aligned}\beta''_k &= -t - \eta_k - \alpha'_k \log(2\eta_k) - \frac{1}{2} \pi \alpha''_k - \pi \sum_{l; \xi_k - \xi_l < 0} \alpha''_l \\ &\quad - \sum_{l \neq k} \alpha''_l \arctan\left(\frac{\eta_k + \eta_l}{\xi_k - \xi_l}\right) \\ &\quad - \frac{1}{2} \sum_{l \neq k} \alpha'_l \log[(\xi_k - \xi_l)^2 + (\eta_k + \eta_l)^2]\end{aligned}\tag{A.20}$$

Note that the in-determination induced by the function \log is made explicit by the multivalued function \arctan . The arguments of the \arctan are real and the first determination Arc tan is finite for any choice of variables.

The unknown functions are the derivatives with respect to time, of the real (ξ_k) part and imaginary (η_k) functions of time-dependent positions of the singularities.

$$\frac{d\xi_k}{dt}, \frac{d\eta_k}{dt} \quad (\text{A.21})$$

Let us introduce systematic standard notations. We note

$$\begin{aligned} X(1) &\equiv \frac{d\xi_1}{dt}, X(2) \equiv \frac{d\xi_2}{dt}, \dots, X(N+1) \equiv \frac{d\xi_{N+1}}{dt}, \\ X(N+2) &\equiv \frac{d\eta_1}{dt}, X(N+3) \equiv \frac{d\eta_2}{dt}, \dots, X(N+1+N+1) \equiv \frac{d\eta_{N+1}}{dt} \end{aligned} \quad (\text{A.22})$$

The variables

$$X(i), \quad \text{for } i = 1, 2N+2 \quad (\text{A.23})$$

are the unknown.

2. The coefficients as result from the equation for the real part ($d\beta'_k/dt = 0$)

We prepare the coefficients in the linear system for $\frac{d\xi_k}{dt}$ and $\frac{d\eta_k}{dt}$ by calculating the derivatives

$$\begin{aligned} &\frac{d}{dt} \arctan \left(\frac{\eta_k + \eta_l}{\xi_k - \xi_l} \right) \\ &= \frac{1}{1 + \left(\frac{\eta_k + \eta_l}{\xi_k - \xi_l} \right)^2} \left[\frac{1}{\xi_k - \xi_l} \left(\frac{d\eta_k}{dt} + \frac{d\eta_l}{dt} \right) - \frac{\eta_k + \eta_l}{(\xi_k - \xi_l)^2} \left(\frac{d\xi_k}{dt} - \frac{d\xi_l}{dt} \right) \right] \\ &= \frac{1}{(\xi_k - \xi_l)^2 + (\eta_k + \eta_l)^2} \left[(\xi_k - \xi_l) \left(\frac{d\eta_k}{dt} + \frac{d\eta_l}{dt} \right) - (\eta_k + \eta_l) \left(\frac{d\xi_k}{dt} - \frac{d\xi_l}{dt} \right) \right] \end{aligned} \quad (\text{A.24})$$

Further

$$\begin{aligned} &\frac{d}{dt} \log [(\xi_k - \xi_l)^2 + (\eta_k + \eta_l)^2] \\ &= \frac{1}{(\xi_k - \xi_l)^2 + (\eta_k + \eta_l)^2} \left[2(\xi_k - \xi_l) \left(\frac{d\xi_k}{dt} - \frac{d\xi_l}{dt} \right) + 2(\eta_k + \eta_l) \left(\frac{d\eta_k}{dt} + \frac{d\eta_l}{dt} \right) \right] \end{aligned} \quad (\text{A.25})$$

and

$$\begin{aligned} \frac{d}{dt} \log(2\eta_k) &= \frac{d}{dt} [\log(\eta_k) + \log(2)] \\ &= \frac{1}{\eta_k} \frac{d\eta_k}{dt} \end{aligned} \quad (\text{A.26})$$

Then we write

$$\begin{aligned}
& \frac{d\beta'_k}{dt} \\
&= \frac{d\xi_k}{dt} \\
& - \sum_{l \neq k} \alpha'_l \frac{1}{(\xi_k - \xi_l)^2 + (\eta_k + \eta_l)^2} \left[(\xi_k - \xi_l) \left(\frac{d\eta_k}{dt} + \frac{d\eta_l}{dt} \right) - (\eta_k + \eta_l) \left(\frac{d\xi_k}{dt} - \frac{d\xi_l}{dt} \right) \right] \\
& + \alpha''_k \frac{1}{\eta_k} \frac{d\eta_k}{dt} \\
& + \frac{1}{2} \sum_{l \neq k} \alpha''_l \frac{1}{(\xi_k - \xi_l)^2 + (\eta_k + \eta_l)^2} \left[2(\xi_k - \xi_l) \left(\frac{d\xi_k}{dt} - \frac{d\xi_l}{dt} \right) + 2(\eta_k + \eta_l) \left(\frac{d\eta_k}{dt} + \frac{d\eta_l}{dt} \right) \right]
\end{aligned} \tag{A.27}$$

In Eq. k . For $k = 1, N + 1$.

Coefficient of $\frac{d\xi_k}{dt}$ is

$$\begin{aligned}
& 1 + \\
& - \sum_{l \neq k} \alpha'_l \frac{1}{(\xi_k - \xi_l)^2 + (\eta_k + \eta_l)^2} [-(\eta_k + \eta_l)] \\
& + \sum_{l \neq k} \alpha''_l \frac{1}{(\xi_k - \xi_l)^2 + (\eta_k + \eta_l)^2} [(\xi_k - \xi_l)]
\end{aligned} \tag{A.28}$$

Coefficient of $\frac{d\xi_l}{dt}$, for $l = 1, N + 1$ but $l \neq k$; it is

$$\begin{aligned}
& -\alpha'_l \frac{1}{(\xi_k - \xi_l)^2 + (\eta_k + \eta_l)^2} [(\eta_k + \eta_l)] \\
& + \alpha''_l \frac{1}{(\xi_k - \xi_l)^2 + (\eta_k + \eta_l)^2} [-(\xi_k - \xi_l)]
\end{aligned} \tag{A.29}$$

Coefficient of $\frac{d\eta_k}{dt}$; this means the the subscript of η_l is the same as the number of the line k . The coefficient is

$$\begin{aligned}
& - \sum_{l \neq k} \alpha'_l \frac{1}{(\xi_k - \xi_l)^2 + (\eta_k + \eta_l)^2} [(\xi_k - \xi_l)] \\
& + \alpha''_k \frac{1}{\eta_k} \\
& + \sum_{l \neq k} \alpha''_l \frac{1}{(\xi_k - \xi_l)^2 + (\eta_k + \eta_l)^2} [(\eta_k + \eta_l)]
\end{aligned} \tag{A.30}$$

Coefficient of $\frac{d\eta_l}{dt}$; for $l = 1, N + 1$ with the constraint $l \neq k$; the subscript of η_l is different from the number of the line k . The coefficient is

$$\begin{aligned}
& -\alpha'_l \frac{1}{(\xi_k - \xi_l)^2 + (\eta_k + \eta_l)^2} [(\xi_k - \xi_l)] \\
& + \alpha''_l \frac{1}{(\xi_k - \xi_l)^2 + (\eta_k + \eta_l)^2} [(\eta_k + \eta_l)]
\end{aligned} \tag{A.31}$$

Free term; it is 0.

a. *The list of types of coefficients.* We note that there are few types.

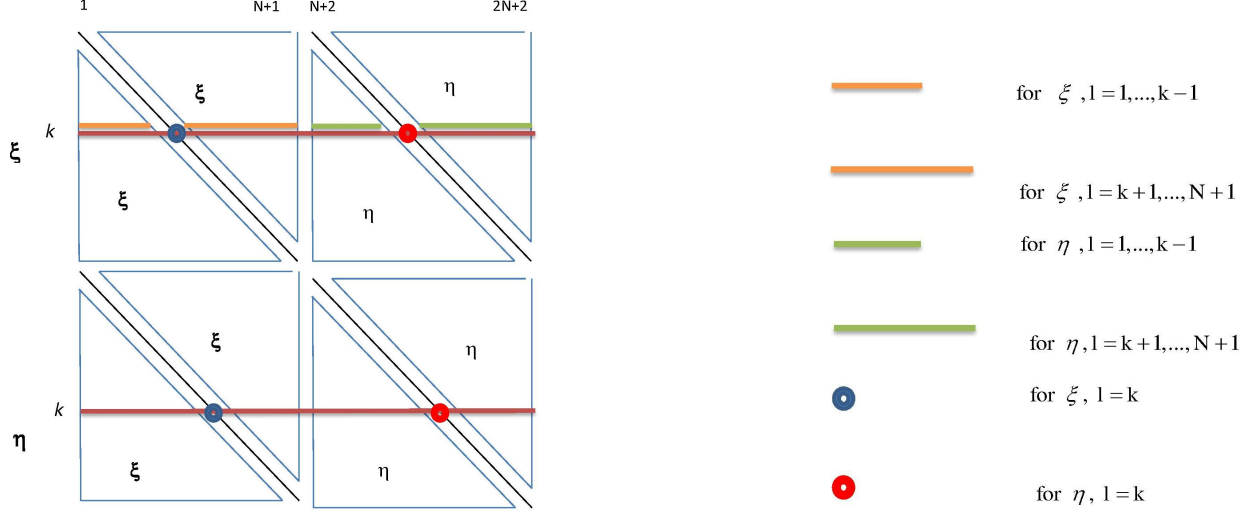


Figure 15: The schematic representation of the matrix of the system.

First divide the full $(2N + 2) \times (2N + 2)$ matrix into four squares each of $(N + 1) \times (N + 1)$.

There are 6 regions along a line of the matrix $A(I, J)$.

the number of types is however less due to repetitions.

We note that the coefficients for line I , coming from $\frac{d\xi_I}{dt}$ but for $J \neq I$ is one type. They are to be found for “columns” J that are in the first Jacobi square matrix

$$1 \leq I \leq N + 1, 1 \leq J \leq N + 1 \quad (\text{A.32})$$

The first part is

$$1 \leq I \leq N + 1, 1 \leq J < I \quad (\text{A.33})$$

This is the type $W1(k, l)$. The expression is

$$\begin{aligned} W1(k, l) = & \quad (\text{A.34}) \\ & -\alpha'_l \frac{1}{(\xi_k - \xi_l)^2 + (\eta_k + \eta_l)^2} [(\eta_k + \eta_l)] \\ & +\alpha''_l \frac{1}{(\xi_k - \xi_l)^2 + (\eta_k + \eta_l)^2} [-(\xi_k - \xi_l)] \end{aligned}$$

where

$$k = I \tag{A.35}$$

$$l = J$$

Then we have a different expression for the local diagonal $J = I$.

$$J = I \tag{A.36}$$

This type is $W2(k, k)$. The expression is

$$W2(k, k) = \tag{A.37}$$

$$\begin{aligned} & 1 + \\ & - \sum_{l \neq k} \alpha'_l \frac{1}{(\xi_k - \xi_l)^2 + (\eta_k + \eta_l)^2} [- (\eta_k + \eta_l)] \\ & + \sum_{l \neq k} \alpha''_l \frac{1}{(\xi_k - \xi_l)^2 + (\eta_k + \eta_l)^2} [(\xi_k - \xi_l)] \end{aligned}$$

where

$$k = I = J \tag{A.38}$$

Along the line, for columns less than $J = N + 1$ which is the end of the first square,

$$1 \leq I \leq N + 1, \quad I + 1 \leq J \leq N + 1 \tag{A.39}$$

the type is again $W1(k, l)$.

$$W1(k, l) = \tag{A.40}$$

$$\begin{aligned} & - \alpha'_l \frac{1}{(\xi_k - \xi_l)^2 + (\eta_k + \eta_l)^2} [(\eta_k + \eta_l)] \\ & + \alpha''_l \frac{1}{(\xi_k - \xi_l)^2 + (\eta_k + \eta_l)^2} [- (\xi_k - \xi_l)] \end{aligned}$$

where

$$k = I \tag{A.41}$$

$$l = J$$

Along the line I , we now go to the second square

$$1 \leq I \leq N + 1, \quad (N + 1) + 1 \leq J \leq (N + 1) + N + 1 \tag{A.42}$$

These columns come from $\frac{d\eta_I}{dt}$. Here again we have to make the difference between $J \neq I$ and $J = I$.

For the first columns, before the local diagonal,

$$1 \leq I \leq N + 1, (N + 1) + 1 \leq J < (N + 1) + I \quad (\text{A.43})$$

the type is $W3(I, J)$. The expression is adapted to this range of indices.

$$\begin{aligned} W3(k, l) = & \quad (\text{A.44}) \\ & -\alpha'_l \frac{1}{(\xi_k - \xi_l)^2 + (\eta_k + \eta_l)^2} [(\xi_k - \xi_l)] \\ & +\alpha''_l \frac{1}{(\xi_k - \xi_l)^2 + (\eta_k + \eta_l)^2} [(\eta_k + \eta_l)] \end{aligned}$$

with

$$\begin{aligned} k &= I & (\text{A.45}) \\ l &= J - (N + 1) \end{aligned}$$

Then comes the local diagonal in this square matrix

$$1 \leq I \leq N + 1, \text{ with } J - (N + 1) = I \quad (\text{A.46})$$

$$\text{for } (N + 1) + 1 \leq J \leq (N + 1) + N + 1$$

This is type $W4(k, l)$. The expression is

$$\begin{aligned} W4(k, k) = & \quad (\text{A.47}) \\ & -\sum_{l \neq k} \alpha'_l \frac{1}{(\xi_k - \xi_l)^2 + (\eta_k + \eta_l)^2} [(\xi_k - \xi_l)] \\ & +\alpha''_k \frac{1}{\eta_k} \\ & +\sum_{l \neq k} \alpha''_l \frac{1}{(\xi_k - \xi_l)^2 + (\eta_k + \eta_l)^2} [(\eta_k + \eta_l)] \end{aligned}$$

where

$$k = I = J - (N + 1) \quad (\text{A.48})$$

Next along the same line I ,

$$1 \leq I \leq N + 1, (N + 1) + I + 1 \leq J \leq (N + 1) + N + 1 \quad (\text{A.49})$$

the type is again $W3(k, l)$. The expression is

$$\begin{aligned}
W3(k, l) = & \tag{A.50} \\
& -\alpha'_l \frac{1}{(\xi_k - \xi_l)^2 + (\eta_k + \eta_l)^2} [(\xi_k - \xi_l)] \\
& +\alpha''_l \frac{1}{(\xi_k - \xi_l)^2 + (\eta_k + \eta_l)^2} [(\eta_k + \eta_l)]
\end{aligned}$$

where

$$\begin{aligned}
k &= I \tag{A.51} \\
l &= J - (N + 1)
\end{aligned}$$

for the range (I, J) written above.

Let us consider application to few lines.

b. The line for the unknown $X(1)$. This is $\frac{d\xi_1}{dt}$.

The first case consists of: the indice (l) of the coefficient coincides with the number of the line (which is $k = 1$).

This first case is the diagonal element. It comes from $\frac{d\xi_1}{dt}$. The model is $W2(k, k)$ for $k = I = 1$.

$$\begin{aligned}
A(1, 1) = & \tag{A.52} \\
& 1 + \\
& - \sum_{l \neq 1}^{N+1} \alpha'_l \frac{1}{(\xi_1 - \xi_l)^2 + (\eta_1 + \eta_l)^2} [-(\eta_1 + \eta_l)] \\
& + \sum_{l \neq 1}^{N+1} \alpha''_l \frac{1}{(\xi_1 - \xi_l)^2 + (\eta_1 + \eta_l)^2} [(\xi_1 - \xi_l)]
\end{aligned}$$

The other cases of entries coming from $\frac{d\xi_l}{dt}$ have the indice of the matrix entry (coefficient, l) different of the number of the line ($k = 1$).

They are non-diagonal elements, upper to local diagonal (which in this particular case is the main diagonal); first N non-diagonal - upper - elements. They come from $\frac{d\xi_l}{dt}$, for $l \neq 1$. The model is $W1(I, J)$, for $I = 1$ and $I + 1 \leq J \leq N + 1$.

$$\begin{aligned}
A(1, J) = & \tag{A.53} \\
& -\alpha'_J \frac{1}{(\xi_1 - \xi_J)^2 + (\eta_1 + \eta_J)^2} [(\eta_1 + \eta_J)] \\
& +\alpha''_J \frac{1}{(\xi_1 - \xi_J)^2 + (\eta_1 + \eta_J)^2} [-(\xi_1 - \xi_J)]
\end{aligned}$$

Next $N + 1$ entries on the first line originate from $\frac{d\eta_l}{dt}$.

The real position in the line of must be found by adding to its indice l of $\frac{d\eta_l}{dt}$ the number of coefficients already considered, $N + 1$.

They are classified according to the same criterium. The indice (l) is equal or not with the number of the line ($k = 1$).

The first case is $l = k = 1$, the indice is equal to the number of the line. It comes from $\frac{d\eta_1}{dt}$. The model is $W4(k, l)$, adapted for the second indice to be returned to the $l = I$.

$$\begin{aligned}
A(1, N + 1 + 1) = & \hspace{15em} (A.54) \\
& \alpha_1'' \frac{1}{\eta_1} \\
- \sum_{l \neq 1} \alpha_l' & \frac{1}{(\xi_1 - \xi_l)^2 + (\eta_1 + \eta_l)^2} [(\xi_1 - \xi_l)] \\
+ \sum_{l \neq 1} \alpha_l'' & \frac{1}{(\xi_1 - \xi_l)^2 + (\eta_1 + \eta_l)^2} [(\eta_1 + \eta_l)]
\end{aligned}$$

which means $A(1, N + 2)$.

The next N come from $\frac{d\eta_l}{dt}$. The indice l is NOT equal with the number of the line $k = 1$. The type is again $W3(k, l)$ adapted for

$$I = 1 \text{ and } (N + 1) + 1 \leq J \leq (N + 1) + N + 1 \quad (A.55)$$

with

$$\begin{aligned}
A(1, N + 1 + l) = & \hspace{15em} (A.56) \\
- \alpha_l' & \frac{1}{(\xi_1 - \xi_l)^2 + (\eta_1 + \eta_l)^2} [(\xi_1 - \xi_l)] \\
+ \alpha_l'' & \frac{1}{(\xi_1 - \xi_l)^2 + (\eta_1 + \eta_l)^2} [(\eta_1 + \eta_l)]
\end{aligned}$$

for $l = 2, N + 1$, which means $A(1, N + 3), \dots, A(1, 2N + 2)$.

c. The line for the unknown $X(2)$. The first elements are non-diagonal elements; here are the lower part.

For this case the indice l is NOT equal with the number of the line $k = 2$.

They come from $\frac{d\xi_l}{dt}$ for $l = 1, 2 - 1$. This means $\frac{d\xi_1}{dt}$, a unique element. The type is $W1(I, J)$ adapted for $I = 2$ and $J = 1$.

$$\begin{aligned}
A(2, l) = & \tag{A.57} \\
& -\alpha'_l \frac{1}{(\xi_2 - \xi_l)^2 + (\eta_2 + \eta_l)^2} [(\eta_2 + \eta_l)] \\
& +\alpha''_l \frac{1}{(\xi_2 - \xi_l)^2 + (\eta_2 + \eta_l)^2} [-(\xi_2 - \xi_l)]
\end{aligned}$$

for $l = 1, \dots, 1$, a single value.

Next entry consists of the case where the indice l of the entry (coefficient) coincides with the number of the line $k = 2$.

The diagonal element. It comes from $\frac{d\xi_2}{dt}$. The type is $W2(I, J)$ for $J = I = 2$.

$$\begin{aligned}
A(2, 2) = & \tag{A.58} \\
& 1 + \\
& - \sum_{l \neq 2} \alpha'_l \frac{1}{(\xi_2 - \xi_l)^2 + (\eta_2 + \eta_l)^2} [-(\eta_2 + \eta_l)] \\
& + \sum_{l \neq 2} \alpha''_l \frac{1}{(\xi_2 - \xi_l)^2 + (\eta_2 + \eta_l)^2} [(\xi_2 - \xi_l)]
\end{aligned}$$

Next cases are still coming from the set $\frac{d\xi_l}{dt}$ but their indice l does not coincide with the number of the line $k = 2$, it is greater than $k = 2$. The type is again $W1(I, J)$ for $J > I = 2$.

$$\begin{aligned}
A(2, l) = & \tag{A.59} \\
& -\alpha'_l \frac{1}{(\xi_2 - \xi_l)^2 + (\eta_2 + \eta_l)^2} [(\eta_2 + \eta_l)] \\
& +\alpha''_l \frac{1}{(\xi_2 - \xi_l)^2 + (\eta_2 + \eta_l)^2} [-(\xi_2 - \xi_l)]
\end{aligned}$$

Their number is $l = 2 + 1, \dots, N + 1$ which is $l = 3, N + 1$.

Next entries (coefficients) are upper diagonal elements and come from $\frac{d\eta_l}{dt}$.

We must make difference between (1) $l = 1, \dots, N + 1$ but $l \neq 2$ and (2) $l = 2$, where the index l only refers to $\frac{d\eta_l}{dt}$. The indices for the full matrix are calculated adding $N + 1$, corresponding to all the positions occupied by $\frac{d\xi_l}{dt}$.

The first case consists of the entries coming from $\frac{d\eta_l}{dt}$ with l less than the number of the line $k = 2$. The type of these terms is $W3(I, J)$, for $J - (N + 1) < I$. This group here only

contains one element, since we are at the line 2. Then $l = 1$. This coefficient comes from $\frac{d\eta_1}{dt}$.

$$\begin{aligned}
A(2, N + 1 + 1) = & \tag{A.60} \\
& -\alpha'_1 \frac{1}{(\xi_2 - \xi_1)^2 + (\eta_2 + \eta_1)^2} [(\xi_2 - \xi_1)] \\
& +\alpha''_1 \frac{1}{(\xi_2 - \xi_1)^2 + (\eta_2 + \eta_1)^2} [(\eta_2 + \eta_1)]
\end{aligned}$$

It follows the entry coming from $\frac{d\eta_l}{dt}$ with the indice l coinciding with the number of the line $k = 2$, *i.e.* $l = k = 2$. It comes from $\frac{d\eta_2}{dt}$. The type is $W4(I, I)$.

$$\begin{aligned}
A(2, N + 1 + l) = A(2, N + 1 + 2) = & \tag{A.61} \\
& \alpha''_2 \frac{1}{\eta_2} \\
& - \sum_{l \neq 2}^{N+1} \alpha'_l \frac{1}{(\xi_2 - \xi_l)^2 + (\eta_2 + \eta_l)^2} [(\xi_2 - \xi_l)] \\
& + \sum_{l \neq 2}^{N+1} \alpha''_l \frac{1}{(\xi_2 - \xi_l)^2 + (\eta_2 + \eta_l)^2} [(\eta_2 + \eta_l)]
\end{aligned}$$

The next group contains all other coefficients coming from $\frac{d\eta_l}{dt}$ whose indice l does not coincide with the number of the line (*i.e.* $k = 2$). This means for $l = 3, \dots, N + 1$. The indice will be produced by adding $l = 3, \dots, N + 1$ to $N + 1$ (already taken by $\frac{d\xi_l}{dt}$). The type is again $W3(I, J)$ for $I = 2$ and $(N + 1) + 1 < J$.

$$\begin{aligned}
A(2, N + 1 + l) = & \text{(only for } l = 3, \dots, N + 1) \tag{A.62} \\
& -\alpha'_l \frac{1}{(\xi_2 - \xi_l)^2 + (\eta_2 + \eta_l)^2} [(\xi_2 - \xi_l)] \\
& +\alpha''_l \frac{1}{(\xi_2 - \xi_l)^2 + (\eta_2 + \eta_l)^2} [(\eta_2 + \eta_l)]
\end{aligned}$$

This fills all entries on the line $k = 2$. The two exercises (for $k = 1, 2$) can be used as a check for the computer code.

3. The coefficients resulting from the equation for the imaginary part
($d\beta_k''/dt = 0$)

The time derivative of the imaginary part, β_k'' .

$$\begin{aligned} & \frac{d\beta_k''}{dt} \\ &= -1 - \frac{d\eta_k}{dt} - \alpha'_k \frac{1}{\eta_k} \frac{d\eta_k}{dt} \\ & - \sum_{l \neq k} \alpha_l'' \frac{1}{(\xi_k - \xi_l)^2 + (\eta_k + \eta_l)^2} \left[(\xi_k - \xi_l) \left(\frac{d\eta_k}{dt} + \frac{d\eta_l}{dt} \right) - (\eta_k + \eta_l) \left(\frac{d\xi_k}{dt} - \frac{d\xi_l}{dt} \right) \right] \\ & - \frac{1}{2} \sum_{l \neq k} \alpha_l' \frac{1}{(\xi_k - \xi_l)^2 + (\eta_k + \eta_l)^2} \left[2(\xi_k - \xi_l) \left(\frac{d\xi_k}{dt} - \frac{d\xi_l}{dt} \right) + 2(\eta_k + \eta_l) \left(\frac{d\eta_k}{dt} + \frac{d\eta_l}{dt} \right) \right] \end{aligned} \quad (\text{A.63})$$

In Eq. k . For $k = 1, N + 1$.

Coefficient of $\frac{d\xi_k}{dt}$ is

$$\begin{aligned} & - \sum_{l \neq k} \alpha_l'' \frac{1}{(\xi_k - \xi_l)^2 + (\eta_k + \eta_l)^2} [-(\eta_k + \eta_l)] \\ & - \sum_{l \neq k} \alpha_l' \frac{1}{(\xi_k - \xi_l)^2 + (\eta_k + \eta_l)^2} [(\xi_k - \xi_l)] \end{aligned} \quad (\text{A.64})$$

Coefficient of $\frac{d\xi_l}{dt}$. For $l = 1, N + 1$, but $l \neq k$.

$$\begin{aligned} & - \alpha_l'' \frac{1}{(\xi_k - \xi_l)^2 + (\eta_k + \eta_l)^2} [(\eta_k + \eta_l)] \\ & - \alpha_l' \frac{1}{(\xi_k - \xi_l)^2 + (\eta_k + \eta_l)^2} [-(\xi_k - \xi_l)] \end{aligned} \quad (\text{A.65})$$

Coefficient of $\frac{d\eta_k}{dt}$; it is

$$\begin{aligned} & -1 - \alpha'_k \frac{1}{\eta_k} \\ & - \sum_{l \neq k} \alpha_l'' \frac{1}{(\xi_k - \xi_l)^2 + (\eta_k + \eta_l)^2} [(\xi_k - \xi_l)] \\ & - \sum_{l \neq k} \alpha_l' \frac{1}{(\xi_k - \xi_l)^2 + (\eta_k + \eta_l)^2} [(\eta_k + \eta_l)] \end{aligned} \quad (\text{A.66})$$

Coefficient of $\frac{d\eta_l}{dt}$; it is

$$\begin{aligned} & - \alpha_l'' \frac{1}{(\xi_k - \xi_l)^2 + (\eta_k + \eta_l)^2} [(\xi_k - \xi_l)] \\ & - \alpha_l' \frac{1}{(\xi_k - \xi_l)^2 + (\eta_k + \eta_l)^2} [(\eta_k + \eta_l)] \end{aligned} \quad (\text{A.67})$$

for $l = 1, N + 1$, but $l \neq k$.

The free term; it is, after transferring it to the right side 1 which comes from all equations of β_k'' .

a. *The list of types of coefficients as result from the time derivation of the imaginary part ($d\beta_k''/dt = 0$)* There are 6 regions and the types are also only 4.

Consider the line I , which must be

$$(N + 1) + 1 \leq I \leq (N + 1) + N + 1 \quad (\text{A.68})$$

The first columns J are from $\frac{d\xi_I}{dt}$ which are under the local diagonal. The type is $\Omega 1(k, l)$,

$$\begin{aligned} \Omega 1(k, l) = & \quad (\text{A.69}) \\ & -\alpha_J'' \frac{1}{(\xi_k - \xi_l)^2 + (\eta_k + \eta_l)^2} [(\eta_k + \eta_l)] \\ & -\alpha_J' \frac{1}{(\xi_k - \xi_l)^2 + (\eta_k + \eta_l)^2} [-(\xi_k - \xi_l)] \end{aligned}$$

where the indice k of the variables is I adapted by subtracting the $(N + 1)$ lines of the first Jacobi square.

$$\begin{aligned} k &= I - (N + 1) & (\text{A.70}) \\ l &= J \end{aligned}$$

The range of the indices is

$$\begin{aligned} (N + 1) + 1 &< I \leq (N + 1) + N + 1 & (\text{A.71}) \\ 1 &\leq J < I - (N + 1) \end{aligned}$$

The element that is on the local diagonal has

$$I - (N + 1) = J \quad (\text{A.72})$$

It corresponds to $\frac{d\xi_J}{dt}$ on the line I , with the property $J = I - (N + 1)$. The type is $\Omega 2(I, J)$ with the expression

$$\begin{aligned} \Omega 2(k, k) = & \quad (\text{A.73}) \\ & -\sum_{l \neq k} \alpha_l'' \frac{1}{(\xi_k - \xi_l)^2 + (\eta_k + \eta_l)^2} [-(\eta_k + \eta_l)] \\ & -\sum_{l \neq k} \alpha_l' \frac{1}{(\xi_k - \xi_l)^2 + (\eta_k + \eta_l)^2} [(\xi_k - \xi_l)] \end{aligned}$$

with

$$k = I - (N + 1) \quad (\text{A.74})$$

The range of the indices is

$$\begin{aligned} (N + 1) + 1 < I \leq (N + 1) + N + 1 \\ J = I - (N + 1) \end{aligned} \quad (\text{A.75})$$

For columns that are beyond the local diagonal but still in the third square matrix. they come from $\frac{d\xi_l}{dt}$.

The type is again $\Omega 1(I, J)$ with the expression

$$\begin{aligned} \Omega 1(k, l) = \\ -\alpha''_J \frac{1}{(\xi_k - \xi_l)^2 + (\eta_k + \eta_l)^2} [(\eta_k + \eta_l)] \\ -\alpha'_J \frac{1}{(\xi_k - \xi_l)^2 + (\eta_k + \eta_l)^2} [-(\xi_k - \xi_l)] \end{aligned} \quad (\text{A.76})$$

The range of indices is

$$\begin{aligned} (N + 1) + 1 \leq I \leq (N + 1) + N + 1 \\ I - (N + 1) < J \leq N + 1 \end{aligned} \quad (\text{A.77})$$

which are translated into

$$\begin{aligned} k = I - (N + 1) \\ l = J \end{aligned} \quad (\text{A.78})$$

Now we continue along the line no. I into the fourth square.

For an arbitrary line I , the first columns in the fourth square come from $\frac{d\eta_l}{dt}$. They are of the type $\Omega 3(I, J)$ with expression

$$\begin{aligned} \Omega 3(k, l) = \\ -\alpha''_l \frac{1}{(\xi_k - \xi_l)^2 + (\eta_k + \eta_l)^2} [(\xi_k - \xi_l)] \\ -\alpha'_l \frac{1}{(\xi_k - \xi_l)^2 + (\eta_k + \eta_l)^2} [(\eta_k + \eta_l)] \end{aligned} \quad (\text{A.79})$$

where

$$k = I - (N + 1) \quad (\text{A.80})$$

$$l = J - (N + 1)$$

with the range of the parameters

$$(N + 1) + 1 \leq I \leq (N + 1) + N + 1 \quad (\text{A.81})$$

$$(N + 1) + 1 \leq J < I$$

The element on the local diagonal comes from $\frac{d\eta_I}{dt}$ and the type is $\Omega 4(I, J)$. the expression is

$$\Omega 4(k, k) = \quad (\text{A.82})$$

$$\begin{aligned} & -1 - \alpha'_k \frac{1}{\eta_k} \\ & - \sum_{l \neq k} \alpha''_l \frac{1}{(\xi_k - \xi_l)^2 + (\eta_k + \eta_l)^2} [(\xi_k - \xi_l)] \\ & - \sum_{l \neq k} \alpha'_l \frac{1}{(\xi_k - \xi_l)^2 + (\eta_k + \eta_l)^2} [(\eta_k + \eta_l)] \end{aligned}$$

with

$$k = I - (N + 1) = J - (N + 1) \quad (\text{A.83})$$

and the range

$$(N + 1) + 1 \leq I \leq (N + 1) + N + 1 \quad (\text{A.84})$$

$$J = I$$

Finally we have along the same line (I) the group of columns that are upper the local diagonal in the fourth square.

They come from $\frac{d\eta_I}{dt}$. They are of the $\Omega 3(I, J)$ type again. The expression is

$$\Omega 3(k, l) = \quad (\text{A.85})$$

$$\begin{aligned} & -\alpha''_l \frac{1}{(\xi_k - \xi_l)^2 + (\eta_k + \eta_l)^2} [(\xi_k - \xi_l)] \\ & -\alpha'_l \frac{1}{(\xi_k - \xi_l)^2 + (\eta_k + \eta_l)^2} [(\eta_k + \eta_l)] \end{aligned}$$

The indices are

$$k = I - (N + 1) \tag{A.86}$$

$$l = J - (N + 1)$$

and the range of indices is

$$(N + 1) + 1 \leq I \leq (N + 1) + N + 1 \tag{A.87}$$

$$I < J \leq (N + 1) + N + 1$$

b. The free term in the linear system of equations The free term is

$$F(I) = \begin{cases} 0 & \text{for } 1 \leq I \leq N + 1 \\ +1 & \text{for } (N + 1) + 1 \leq I \leq (N + 1) + N + 1 \end{cases} \tag{A.88}$$

4. The numerical implementation of the time evolution of the positions of the singularities

Assume that we work with $N + 1$ singularities (in the circular case, there are N singularities, in the infinite case there are $N + 1$ singularities).

$$\xi_k + i\eta_k \quad \text{for } k = 1, \dots, N + 1 \tag{A.89}$$

The equations that we intend to solve are of general form

$$\frac{d\xi_k}{dt} = \Xi(\xi_l, \eta_l) \tag{A.90}$$

$$\frac{d\eta_k}{dt} = \Psi(\xi_l, \eta_l)$$

for $k = 1, \dots, N + 1$. Putting together the real and imaginary parts (ξ_k, η_k) as independent unknown variables, the system in the form

$$\sum_{j=1, 2N+2} A(I, J) X(J) = F(I) \tag{A.91}$$

for $I = 1, 2N + 2$

The expressions of $A(I, J)$ depend of (ξ_k, η_k) . Then we can see the sequence

1. we start with a set of variables

$$(\xi_k, \eta_k) \quad , \quad k = 1, 2N + 2 \tag{A.92}$$

2. calculate the matrix

$$A(I, J) \tag{A.93}$$

and the free term

$$F(I) \tag{A.94}$$

3. solve the linear system

$$X(I) = A^{-1}(I, J) F(J) \tag{A.95}$$

4. integrate in time using Runge-Kutta method the system of equations

$$\frac{d\zeta_k}{dt} = X(I) \tag{A.96}$$

and find the new set (ξ_k, η_k) at the time $t + \delta t$.

5. find the current interface $\Gamma(t)$

6. iterate to point 2.

Numerical studies consists of the inversion of the matrix equation

$$AX = F \tag{A.97}$$

followed by time advancement using the Runge Kutta method (the **d02pdf** NAG routine).

C. The time evolution of the mapping function $f(z, t)$

Integrating Eqs.(A.96) we determine the positions of the singularities $\zeta_k(t)$, $k = 1, \dots, N + 1$, as function of time. Now we calculate

$$\begin{aligned} f(z, t) = & z - it \\ & -i \sum_{l=1}^{N+1} (\alpha'_l + i\alpha''_l) \\ & \times \{ \log(|x - \xi_l + iy - i\eta_l|) + i \arg(x - \xi_l + iy - i\eta_l) \} \end{aligned} \tag{A.98}$$

It has been shown^{23, 8, 27} that: if at $t = 0$ all imaginary parts of the singularities of the log function are positive

$$\eta_l > 0 \text{ for } \forall l \tag{A.99}$$

and all constants α_l are real and positive

$$\alpha_l \in \mathbf{R} \tag{A.100}$$

$$\alpha_l > 0 \text{ for } \forall l$$

then the imaginary parts of the zeros y_l and of the singularities η_l remain positive for all time $t > 0$. This preserves the holomorphicity of f .

The *interface line* in the mathematical plane (z) is the straight line which separates the two half-planes $-\infty < x < \infty$, $y = 0$ and it is mapped through the complex function $f(z, t)$ into a *curved line* $\Gamma(t)$ in the real plane of physical variables $X \equiv \mathbf{Re}[f(z, t)]$, $Y \equiv \mathbf{Im}[f(z, t)]$. We can identify the curve that corresponds to the complex line $z = x + i0$ by taking $x \in \mathbf{R}$ and $y = 0$ in the expressions of X, Y .

The general formula for the Real part is

$$\begin{aligned} & \mathbf{Re}[f(z, t)] \tag{A.101} \\ &= x \\ &+ \sum_{l=1}^{N+1} \alpha_l'' \frac{1}{2} \log [(x - \xi_l)^2 + (y - \eta_l)^2] \\ &+ \sum_{l=1}^{N+1} \alpha_l' \arg(x + iy - \xi_l + i\eta_l) \end{aligned}$$

where we choose $\alpha_l'' \equiv 0$ for all l , then $y = 0$.

$$\begin{aligned} & X_0(x, t) \tag{A.102} \\ &= x - \sum_{l=1}^{N+1} \alpha_l' \arg(x - \xi_l + i\eta_l) \end{aligned}$$

Similarly, we have the general form

$$\begin{aligned} & \mathbf{Im}[f(z, t)] \tag{A.103} \\ &= y - t \\ &- \sum_{l=1}^{N+1} \alpha_l' \frac{1}{2} \log [(x - \xi_l)^2 + (y - \eta_l)^2] \\ &+ \sum_{l=1}^{N+1} \alpha_l'' \arg(x + iy - \xi_l + i\eta_l) \end{aligned}$$

and take $\alpha'_l \equiv 0$ and $y = 0$

$$Y_0(x, t) = -t - \sum_{l=1}^{N+1} \alpha'_l \frac{1}{2} \log [(x - \xi_l)^2 + (y - \eta_l)^2] \quad (\text{A.104})$$

The interface is formally defined as

$$\Gamma(t) = Y_0(X_0, t) \quad (\text{A.105})$$

which means that the variable x is eliminated between $X_0(x, t)$ and $Y_0(x, t)$.

The phase of the logarithm must be contained in

$$0 \leq \arg(x - \xi_l + i\eta_l) \leq \pi \quad (\text{A.106})$$

because $\eta_l > 0$ for $\forall l$. There is nothing special with x traversing the point ξ_l if we think in terms of the vector in complex plane based in the origin $(0, 0)$ and pointing to $(x - \xi_l, \eta_l)$. When $x - \xi_l \equiv -|\varepsilon| < 0$ the vector is almost aligned with the imaginary axis and the angle it makes with the abscissa (the phase of the argument of the logarithm) is slightly greater than $\pi/2$. When x moves to become greater than ξ_l , $x - \xi_l \equiv |\varepsilon| > 0$, the vector is still almost vertical but the angle with the abscissa is slightly less than $\pi/2$. Therefore when x traverses the position ξ_l the phase of the logarithm smoothly changes around $\pi/2$. When the argument of the complex number $(x - \xi_l + i\eta_l)$ is calculated numerically, we must take into account that the function $\arctan \equiv (\tan)^{-1}$ is determined between $-\pi/2$ and $\pi/2$. Consider

$$\eta_l > 0 \quad (\text{which is always true}) \quad (\text{A.107})$$

$$x - \xi_l = +|\varepsilon| \quad (\text{very small})$$

which means that x approaches ξ_l from the right, such that $x - \xi_l > 0$. Then $\arg(x - \xi_l + i\eta_l) \lesssim \frac{\pi}{2}$ which is obtained with the arctan function, since

$$\arctan\left(\frac{\eta_l}{x - \xi_l}\right) = \arctan\left(\frac{\eta_l}{|\varepsilon|}\right) \approx \arctan(+\infty) = \frac{\pi}{2} \quad (\text{A.108})$$

and we can write for this case

$$\arg(x - \xi_l + i\eta_l) = \arctan\left(\frac{\eta_l}{x - \xi_l}\right) \quad (\text{A.109})$$

For the opposite case, where x approaches ξ_l from the left,

$$\begin{aligned}\eta_l &> 0 \\ x - \xi_l &= -|\varepsilon|\end{aligned}\tag{A.110}$$

the value of $\arg(x - \xi_l + i\eta_l)$ is again close to $\pi/2$, $\arg(x - \xi_l + i\eta_l) \gtrsim \frac{\pi}{2}$, but in this case the function \arctan gives

$$\arctan\left(\frac{\eta_l}{-|\varepsilon|}\right) \approx \arctan(-\infty) = -\frac{\pi}{2}\tag{A.111}$$

and if we want to use \arctan to obtain the \arg then we must correct the result, by adding π

$$\arg(x - \xi_l + i\eta_l) = \arctan\left(\frac{\eta_l}{x - \xi_l}\right) + \pi\tag{A.112}$$

The two functions become

$$\begin{aligned}X_0(x, t) &= x \\ &\quad - \sum_{l=1}^{N+1} \alpha'_l \arctan\left(\frac{\eta_l}{x - \xi_l}\right) - \pi \sum_{l; x - \xi_l < 0} \alpha'_l \\ Y_0(x, t) &= -t \\ &\quad - \sum_{l=1}^{N+1} \alpha'_l \frac{1}{2} \log [(x - \xi_l)^2 + (y - \eta_l)^2]\end{aligned}$$

D. Note on the stagnation points

We find that the calculation of the imaginary part

$$Y_0 = -t - \sum_{l=1}^{N+1} \alpha'_l \frac{1}{2} \log [(x - \xi_l)^2 + (y - \eta_l)^2]$$

makes $Y_0(x, t)$ strongly (linearly) dependent of time t . Then apparently the *lines* representing the interface are always substantially shifted one relative to the other and the *stagnation points*⁸ do not appear. However it can be proved that the linear term $-t$ is cancelled by an opposite term arising from the sum in the second term.

The only possibility is that

$$\begin{aligned} x - \xi_l &\rightarrow 0 \\ y &= 0 \text{ this is the interface} \\ \eta_l &\rightarrow \exp\left(-\frac{t}{\alpha'_l}\right) \end{aligned}$$

This would be realized if the set of equations of time evolution of the (ξ_l, η_l) would give
- in the second half, for η_l , the general form

$$A(I, J) \begin{pmatrix} \frac{d\xi_l}{dt} \\ \frac{d\eta_l}{dt} \end{pmatrix} = \begin{pmatrix} 0 \\ 1 \end{pmatrix}$$

or

$$\frac{d\eta_l}{dt} = -\frac{1}{\alpha'_l}\eta_l + \dots$$

The diagonal of the matrix is

$$\begin{aligned} \Omega 4(k, k) &= \\ & -1 - \alpha'_k \frac{1}{\eta_k} \\ & - \sum_{l \neq k} \alpha''_l \frac{1}{(\xi_k - \xi_l)^2 + (\eta_k + \eta_l)^2} [(\xi_k - \xi_l)] \\ & - \sum_{l \neq k} \alpha'_l \frac{1}{(\xi_k - \xi_l)^2 + (\eta_k + \eta_l)^2} [(\eta_k + \eta_l)] \end{aligned}$$

and we can approximate

$$\begin{aligned} \frac{d\eta_l}{dt} &\sim [\Omega 4(l, l)]^{-1} \\ &= \frac{1}{-1 - \alpha'_l \frac{1}{\eta_l} - \dots} \end{aligned}$$

We note that

$$\begin{aligned} \eta_l &\sim \text{very small} \\ &\rightarrow \left| \alpha'_l \frac{1}{\eta_l} \right| \gg 1 \end{aligned}$$

and the first term -1 can be neglected. Then

$$\frac{d\eta_l}{dt} \sim -\frac{1}{\alpha'_l}\eta_l + \dots$$

and the solution is indeed

$$\eta_l(t) \sim \eta_l^{(0)} \exp\left(-\frac{t}{\alpha'_l}\right)$$

(Here we see why α'_l must be > 0).

We know that the singularities have evolved, qualitatively, in this way

- the real parts are approaching one the other but this is a slow process. Approximately the initial positions ξ_l are almost unchanged.
- the imaginary part decreases rapidly, remains positive but approaches zero exponentially fast.

Then we find that when we approach with x the position ξ_l of one of the singularities

$$x - \xi_l \rightarrow 0$$

the term in the sum

$$Y_0 = -t - \sum_{l=1}^{N+1} \alpha'_l \frac{1}{2} \log [(x - \xi_l)^2 + (y - \eta_l)^2]$$

becomes approximately

$$\begin{aligned} Y_0 &\approx -t - \alpha'_l \log \left[\sqrt{(y - \eta_l)^2} \right] \quad \text{where } y = 0 \text{ on the interface} \\ &\approx -t - \alpha'_l \left(-\frac{t}{\alpha'_l} \right) - \alpha'_l \log \left(\eta_l^{(0)} \right) + \dots \\ &\approx \text{const} > 0 \end{aligned}$$

and this means that the tip $[X_0(t), Y_0(t)]$ for $t \rightarrow \infty$, of the curve

$$[\xi_l(t), \eta_l(t)]$$

is almost fixed. These are the *stagnation points*^{8,27}.

We note that the line $\mathbf{Re}[f(z, t)]$ shows small but abrupt changes. These are not singularities however, but they are the result of the finite precision of the representation of the two lines that are mapped by the conformal transformation. Essentially it is the degree of the detail when one approaches a singularity of the complex log function which introduces these jumps.

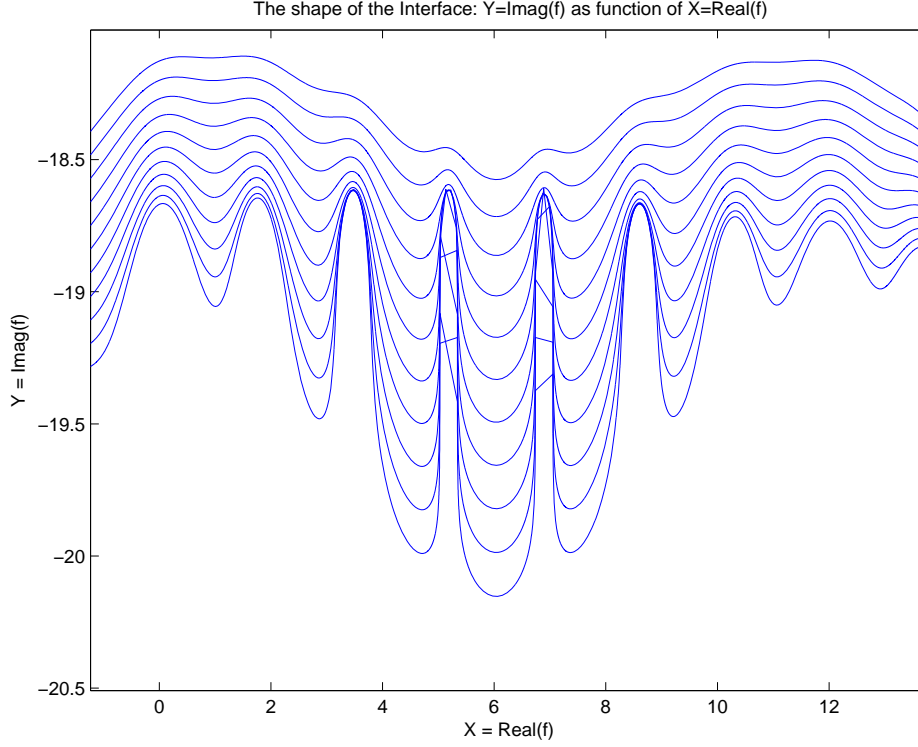


Figure 16: The time variation of the shape of the interface $[X(t), Y(t)]$ for the latest 11 time moments, $t = 90, \dots, 100$. The effect of imprecisions generated by $(x - \xi_l, \eta_l) \rightarrow (0, 0)$ consist of spurious lines that connect the fingers. They are made visible in Fig20.

We explore the regions around the quasi-singularities with *adapted mesh refinement*. The spatial interval is $x \in [x_{\min}, x_{\max}]$ and we choose a number of *average* mesh intervals, M . The *average* mesh interval is $\bar{\delta x} = (x_{\max} - x_{\min})/M$. Now we choose a function $f(x; \xi_l)$ to modulate $\bar{\delta x}$ around a point x . We take

$$f(x; \xi_l) = c + \sum_{l=1}^{NN} a_l \exp \left[-\frac{(x - \xi_l)^2}{2b_l^2} \right]$$

where $c \equiv \text{constant}$, $a_l = \text{amplitude of } f \text{ for } l = 1, NN = N + 1$, the number of singularities ξ_l . $b_l = \text{half-width at inflection point}$. For example, for $M = 1000$, $c = 1$, $a_l = 40$, $b_l = (\xi_{l+1} - \xi_{l-1})/d_l$ and $d_l = \text{constant factor} = 10$, the refined mesh has 9700 intervals. The strongly non-uniform mesh allows a good precision in the regions where $x - \xi - l \sim 0$ but are not able to remove the imprecisions when also $\eta_l \sim 0$. We conclude that special precautions must be taken for the late phase of the time evolution since in this regime η_l becomes very small. In Figs.2, 3 and 4 we have avoided this region.

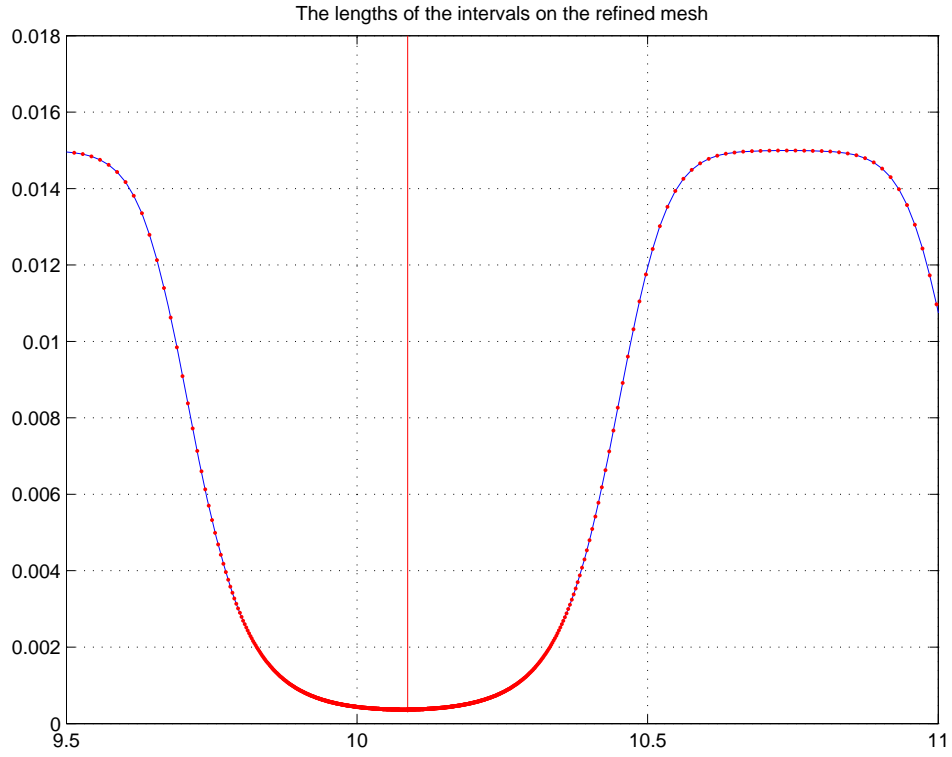


Figure 17: The lengths of the intervals of the refined mesh on the line $x = \mathbf{Re}(z)$ in the “mathematical plane” . The non-uniform distribution is imposed by the need to explore carefully the regions around the quasi-singularities: $(x - \xi_l) \sim 0, \eta_l \sim 0$.

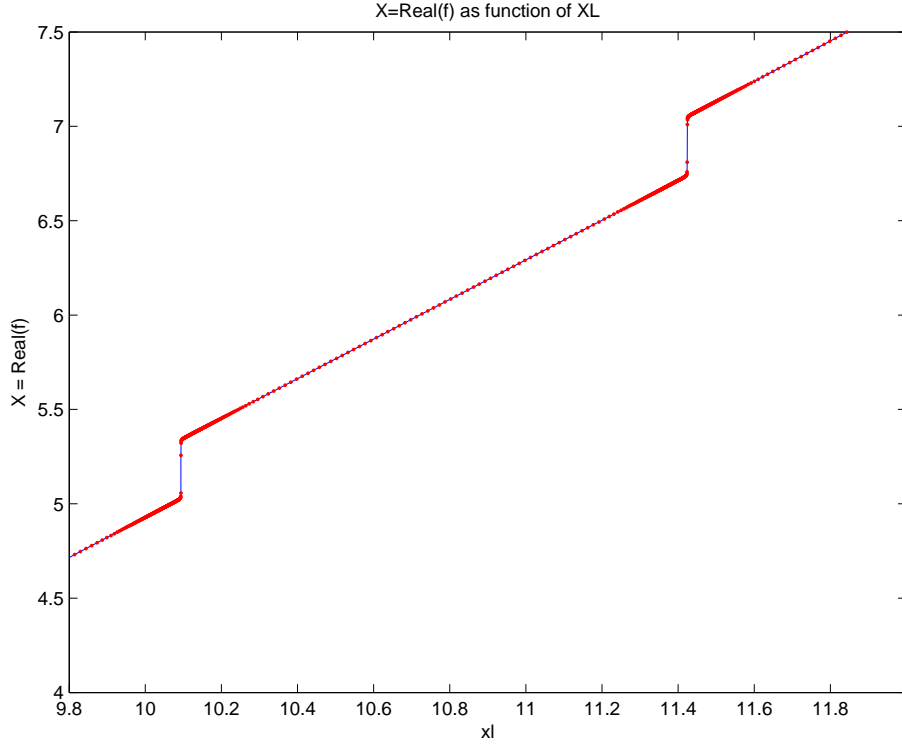


Figure 18: The X coordinate of the points on the interface (*i.e.* $X = \mathbf{Re}[f(z)]$) as function of x , the coordinate of the abscissa on the mathematical plane $z = x + iy$. A small x -interval is plotted, to show the quasi-singular variation of $\mathbf{Re}[f(z)]$ which is due to two situations where we have both $x - \xi_l \rightarrow 0$ and $\eta_l \approx 0$. These cases produce the errors of the interface profile. The result here is for $t = 94$.

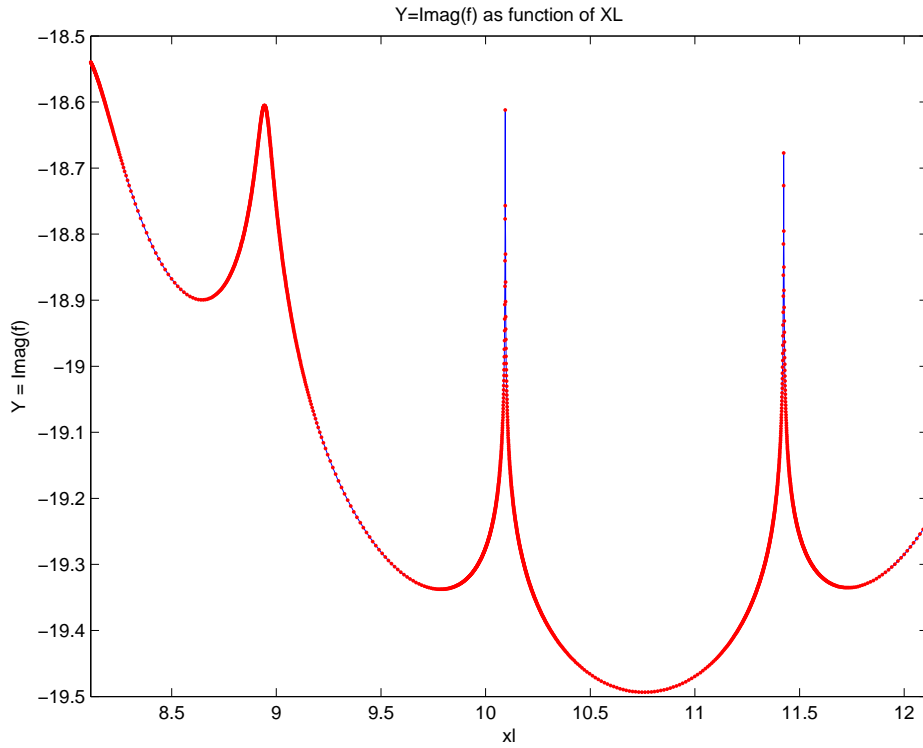


Figure 19: Same as Fig16 but here $Y = \mathbf{Im}[f(z)]$ is plotted. The quasi-singular behavior has the same origin.

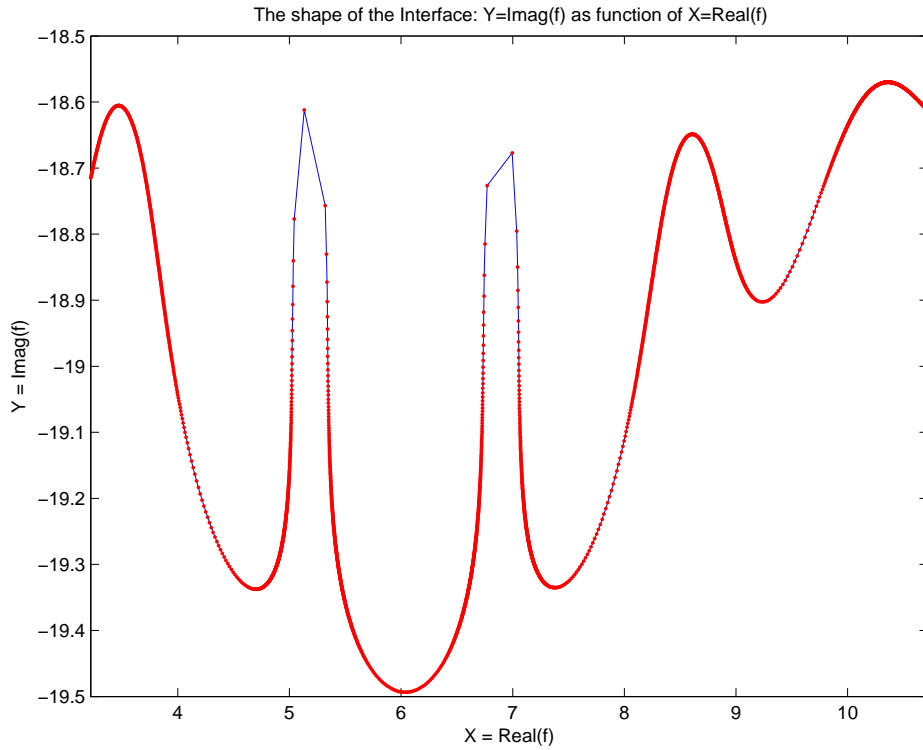


Figure 20: A small region of the interface, from the same results as Figs.18 and 19. Although a high degree of mesh refinement is used, the space variation of the interface is not correctly resolved around the two points shown in Fig.18 and spurious lines are introduced, the same that are seen in Fig.16.

B. APPENDIX. WRINKLED FRONTS AND CUSP SINGULARITIES

For the examination of the cusp profiles, the equation of Sivashinsky type is solved in terms of a set of singularities (poles). The time dependence of the solution is encoded in the dynamics of the poles. The equations verified by the poles are^{24, 19}

$$-L^2 \frac{dz_j}{dt} = \nu \sum_{k=1, k \neq j}^{2N} \cot \left(\frac{z_j - z_k}{2} \right) + i \frac{L}{2} \text{sign} [\mathbf{Im} (z_j)] \quad (\text{B.1})$$

Here the poles are counted all, with the first N indices $j = 1, \dots, N$ for poles and the last N indices $j = N + 1, \dots, 2N$ for the conjugated poles.

$$z_{j+N} = \bar{z}_j \quad (\text{B.2})$$

The equations are written for the real and imaginary parts of the poles

$$z_j(t) = x_j(t) + iy_j(t) \quad (\text{B.3})$$

$$-L^2 \frac{dx_j}{dt} = \nu \sum_{k=1, k \neq j}^N \sin(x_j - x_k) \times \left[\frac{1}{\cosh(y_j - y_k) - \cos(x_j - x_k)} + \frac{1}{\cosh(y_j + y_k) - \cos(x_j - x_k)} \right] \quad (\text{B.4})$$

and

$$L^2 \frac{dy_j}{dt} = \nu \sum_{k=1, k \neq j}^N \left[\frac{\sinh(y_j - y_k)}{\cosh(y_j - y_k) - \cos(x_j - x_k)} + \frac{\sinh(y_j + y_k)}{\cosh(y_j + y_k) - \cos(x_j - x_k)} \right] + \nu \coth(y_j) - L \quad (\text{B.5})$$

These are the equations that are solved numerically.

C. APPENDIX. A NOTE ON THE DISCRETE MODEL FOR THE BREAKING OF A RISING CONVECTIVE COLUMN

The coupled lattice map model that is used to represent the physical process of *phase competition* is implemented numerically. Essentially the discrete nature of the problem (in particular the representation of the Laplacian operator) induces a certain stability of the phases, examined by Oppo and Kapral²⁵. On a two-dimensional square lattice we initialize the field in one of the phases and add a small amplitude noise with smooth profile. They are perturbations of Gaussian *2D* shape, with positions, widths and amplitudes generated randomly. We then start the iteration and note the progress of the phase II into the region occupied initially almost completely by the phase I.

One easily see formation of a spatial oscillation pattern whose characteristic extension is close to the unit cell of the lattice. This is connected with the choice of the diffusion coefficient and of the time advancement and are natural element of the model. We must however remove it if we want to use the evolving pattern of the phases to measure either the length of the interface or the area of the phases. This is a simple numerical operation but introduces a certain imprecision, which should not affect the application of this iterative discrete model to the problem of loss of compacity of rising convective columns.

One can measure various quantities of interest, like the connectivity: how many compact patches of the initial convective column still exist in a horizontal plane; or, the area occupied by one of the phases and respectively, the length of the perimeter of the patches of one phase. For this we use the *contour* function (either Matlab or Fortran) and extract the set of closed curves that are defined by the same level. The dependence with the parameters of the iterative map can be studied, as shown in Fig. 14.

REFERENCES

- ¹Joyce M Aitchison and S.D Howison. Computation of Hele - Shaw flows with free boundaries. *Journal of Computational Physics*, 60(3):376 – 390, 1985.
- ²O.B. Ananin, Yu. A. Bykovskii, E. L Stupitskii, and A. M. Khudaverdyan. Formation of a shock wave structure under conditions of expansion of a laser plasma in a low-density gas. *Sov. J. Quantum Electron*, 17:1474–1475, Nov 1987.

- ³Lisa Bengtsson, Martin Steinheimer, Peter Bechtold, and Jean-Francois Geleyn. A stochastic parametrization for deep convection using cellular automata. *Quarterly Journal of the Royal Meteorological Society*, 139(675):1533–1543, 2013.
- ⁴Alan M. Blyth. Entrainment in cumulus clouds. *Journal of Applied Meteorology*, 32:626–641, 1993.
- ⁵Gatan Borot, Bruno Denet, and Guy Joulin. Resolvent methods for steady premixed flame shapes governed by the Zhdanov Trubnikov equation. *Journal of Statistical Mechanics: Theory and Experiment*, 2012(10):P10023, 2012.
- ⁶Christopher S. Bretherton and Sungsu Park. A new bulk shallow-cumulus model and implications for penetrative entrainment feedback on updraft buoyancy. *Journal of the atmospheric sciences*, 65:2174–2193, 2007.
- ⁷Richard L. Carpenter, Kelvin K. Droegemeier, and Alan M. Blyth. Entrainment and detrainment in numerically simulated cumulus congestus clouds. Part I: General results. *Journal of the Atmospheric Sciences*, 55(23):3417–3432, Dec 1998.
- ⁸Silvina Ponce Dawson and Mark Mineev-Weinstein. Long-time behavior of the n-finger solution of the laplacian growth equation. *Physica D: Nonlinear Phenomena*, 73(4):373 – 387, 1994.
- ⁹L. Filyand, G.I. Sivashinsky, and M.L. Frankel. On self-acceleration of outward propagating wrinkled flames. *Physica D: Nonlinear Phenomena*, 72(12):110 – 118, 1994.
- ¹⁰Uriel Frisch and Rudolf Morf. Intermittency in nonlinear dynamics and singularities at complex times. *Phys. Rev. A*, 23:2673–2705, May 1981.
- ¹¹Raymond E. Goldstein, David J. Muraki, and Dean M. Petrich. Interface proliferation and the growth of labyrinths in a reaction-diffusion system. *Phys. Rev. E*, 53:3933–3957, Apr 1996.
- ¹²Yu. A. Gostintsev, A. G. Istratov, and Yu. V. Shulenin. Self-similar propagation of a free turbulent flame in mixed gas mixtures. *Fizika Goreniya i Vzryva*, 24(5):70–76, 1988.
- ¹³Rama Govindarajan. Universal behavior of entrainment due to coherent structures in turbulent shear flow. *Phys. Rev. Lett.*, 88:134503, Mar 2002.
- ¹⁴S. D. Howison. Complex variable methods in heleshaw moving boundary problems. *European Journal of Applied Mathematics*, 3:209–224, 9 1992.
- ¹⁵Guy Joulin and Bruno Denet. Sivashinsky equation for corrugated flames in the large-wrinkle limit. *Phys. Rev. E*, 78:016315, Jul 2008.

- ¹⁶Guy Joulin and Bruno Denet. Flame wrinkles from the Zhdanov - Trubnikov equation. *Physics Letters A*, 376(22):1797 – 1802, 2012.
- ¹⁷Avraham Klein and Oded Agam. Topological transitions in evaporating thin films. *Journal of Physics A: Mathematical and Theoretical*, 45(35):355003, 2012.
- ¹⁸Joachim Krug and Paul Meakin. Kinetic roughening of laplacian fronts. *Phys. Rev. Lett.*, 66:703–706, Feb 1991.
- ¹⁹Oleg Kupervasser, Zeev Olami, and Itamar Procaccia. Stability analysis of flame fronts: Dynamical systems approach in the complex plane. *Phys. Rev. E*, 59:2587–2593, Mar 1999.
- ²⁰Y C Lee and H H Chen. Nonlinear dynamical models of plasma turbulence. *Physica Scripta*, 1982(T2A):41, 1982.
- ²¹J. I. MacPherson and G. A. Isaac. Turbulent characteristics of some canadian cumulus clouds. *Journal of Applied Meteorology*, 16(1):81–90, Jan 1977.
- ²²D.M. Michelson and G.I. Sivashinsky. Nonlinear analysis of hydrodynamic instability in laminar flames II. Numerical experiments. *Acta Astronautica*, 4(1112):1207 – 1221, 1977.
- ²³Mark B. Mineev-Weinstein and Silvina Ponce Dawson. Class of nonsingular exact solutions for Laplacian pattern formation. *Phys. Rev. E*, 50:R24–R27, Jul 1994.
- ²⁴Zeev Olami, Barak Galanti, Oleg Kupervasser, and Itamar Procaccia. Random noise and pole dynamics in unstable front propagation. *Phys. Rev. E*, 55:2649–2663, Mar 1997.
- ²⁵G-L. Oppo and R. Kapral. Domain growth and nucleation in a discrete bistable system. *Phys. Rev. A*, 36:5820–5831, 12 1987.
- ²⁶I. R. Paluch. The entrainment mechanism in colorado cumuli. *J. Atmos. Sci.*, 36:2467–2478, 1979.
- ²⁷Silvina Ponce Dawson and Mark Mineev-Weinstein. Dynamics of closed interfaces in two-dimensional Laplacian growth. *Phys. Rev. E*, 57:3063–3072, Mar 1998.
- ²⁸Jr. Robert A. Houze. *Cloud dynamics*. Academic Press, San Diego, 1993.
- ²⁹A.P. Siebesma and J.W.M. Cuijpers. Evaluation of parametric assumptions for shallow cumulus convection. *J. Atmos. Sci.*, 52(6):650–666, 1995.
- ³⁰G.I. Sivashinsky. Nonlinear analysis of hydrodynamic instability in laminar flames I. Derivation of basic equations. *Acta Astronautica*, 4(1112):1177 – 1206, 1977.
- ³¹P. Squires. Penetrative downdraughts in cumuli. *Tellus*, 10:381–389, 1958.
- ³²O. Thual, U. Frisch, and M. Henon. Application of pole decomposition to an equation governing the dynamics of wrinkled flame fronts. *J. Physique*, 46:1485–1494, 9 1985.